

Plasma Depletions in the Jovian Magnetosphere: Evidence of Transport and Solar Wind Interaction

RALPH L. McNUTT, JR., PAOLO S. COPPI¹, RICHARD S. SELESNICK, AND BRUNO COPPI

Department of Physics and Center for Space Research, Massachusetts Institute of Technology, Cambridge

A series of plasma voids ("dropouts") was observed by the Plasma Science (PLS) experiment in Jupiter's magnetosphere during the Voyager 2 encounter with that planet. A reexamination of Voyager 2 data has led us to conclude that the dropout phenomenon cannot be a manifestation of a plasma wake produced by Ganymede. Rather, the appearance of the dropouts is attributed to changes in the upstream solar wind conditions and the global state of the magnetosphere; the proximity of Voyager 2 to Ganymede at the time is considered to be coincidental. We suggest that these dropouts are evidence of a state of "bubbling" of the magnetosphere that alternates with "laminar" states in which, as in the case of the Voyager 1 encounter with Jupiter, voids are not present and that these states correspond to different processes by which plasma is transported out of the system. The nature of these states is related to changes in the magnitude of the upstream solar wind ram pressure. In the bubbling state, this pressure is higher than in the laminar state and drives an intermittent instability. The analysis presented is one of the first attempts to introduce, in space physics, recently acquired theoretical notions of the physics of finite- β plasmas of which the Jovian magnetospheric plasma is an important example.

INTRODUCTION

Voyager 2 encountered Jupiter in July 1979. On the inbound trajectory the spacecraft passed within 63,000 km of the Galilean satellite Ganymede at 0714 SCET (spacecraft event time) on July 9. The spacecraft trajectory took Voyager downstream of the moon and below its orbital plane. It was anticipated prior to the encounter that a wake might be formed as Ganymede swept up corotating plasma which was overtaking the moon in its orbit. However, instead of a single plasma void directly behind Ganymede, about a dozen decreases were observed in the thermal plasma density during a period of about 8 hours duration, beginning around 0400 SCET and ending at 1200 SCET. During this time the spacecraft moved 17 R_G normal to Ganymede's orbital plane (1 R_G or Ganymede radius = 2635 km), 26 R_G normal to the plane containing Ganymede and Jupiter's spin axis, and 115 R_G ($= 4.24 R_J$, $1 R_J = 71,398$ km) in the radial direction toward Jupiter [Burlaga *et al.*, 1980].

A schematic of the Jovian system showing the relative locations of Jupiter, the Io plasma tori, Ganymede, and the region in which the depletions of thermal plasma were encountered is shown in Figure 1a. The trajectory and locations of the individual depletions, relative to Jupiter and Ganymede, are depicted in Figure 1b. Thirteen depletions are indicated in this schematic and are noted in the following figures as well; however, variations in the plasma density and other parameters are such that the division between variations and true depletions is somewhat arbitrary. The designation of "depletion" is further complicated in some of the cases owing to time aliasing which appears to occur in some of the individual ion spectra obtained by the Plasma Science (PLS) experiment on Voyager. Nominal times of the depletions are given in Table 1. These are based upon the times that no low-energy ($10 \text{ eV} \leq E \leq 140 \text{ eV}$) electrons were observed by the PLS experiment in its electron

mode. Somewhat different times may be derived from the positive ion data for the less prominent depletions.

Burlaga *et al.* [1980] noted that the durations of the depletions as well as their spacings vary in the PLS data, the mean duration being ~ 10 min and the mean spacing ~ 40 min. The only obvious symmetry in either the detailed structure of the cavities or their location is the position of the first one and the last one with respect to Ganymede along the radial direction from Jupiter. This is the primary reason for thinking that the depletions must be related to the passage of Ganymede through the magnetospheric plasma [Ness *et al.*, 1979; Burlaga *et al.*, 1980].

Signatures of these plasma structures were present in data sets returned by other experiments on Voyager. Magnetic field strength depressions were observed at the edges of more than half of the cavities [Ness *et al.*, 1979], and the > 2.5 Mev proton fluxes measured by the Cosmic Ray (CRS) detector on Voyager were found to be higher inside the cavities than outside, the enhancements occurring abruptly at the cavity boundaries [Burlaga *et al.*, 1980]. However, similar structures also occur in the magnetometer data where no plasma depletions are evident, so the overall picture is somewhat confused [Khurana and Kivelson, 1985].

The Low Energy Charged Particle Experiment (LECP) detected a pattern of variations in ion intensities in the range of 0.5 to 4.01 MeV [Armstrong *et al.*, 1981, Krimigis *et al.*, 1979]. These variations in the ion spectra have since been examined in some detail [Tariq *et al.*, 1983] and used to support the earlier hypothesis of Burlaga *et al.* [1980] that the plasma depletions and associated MeV ion variations are indeed plasma signatures produced by the interaction of Ganymede with the Jovian magnetosphere [Tariq *et al.*, 1985]. However, as we note below, there are quantitative problems with their models of the interaction.

As with the magnetic field measurements, there is no signature in the LECP data which directly correlates with all of the depletions observed by the PLS experiment. In particular, Tariq *et al.* [1983] examined in detail positive ion fluxes between 0.215 MeV and 3.50 MeV (energies corresponding to protons; if the detected ions were oxygen or sulfur these would

¹Now at Department of Physics, California Institute of Technology, Pasadena, California.

Copyright 1987 by the American Geophysical Union.

Paper number 6A8636.
0148-0227/87/006A-8636\$05.00

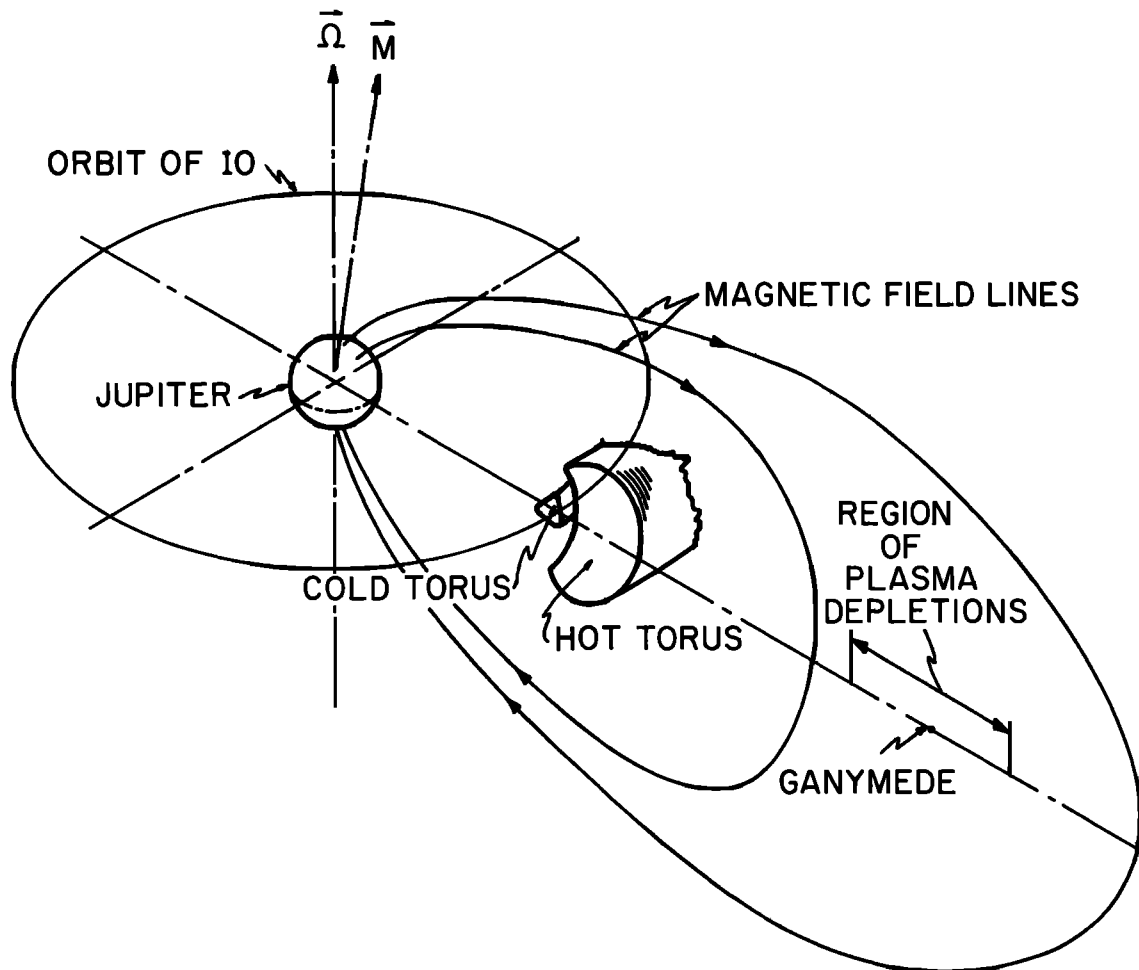


Fig. 1a. Schematic showing the locations of Jupiter, the Io plasma tori, Ganymede, and the region of plasma depletions. The magnetic and spin axes of Jupiter are also indicated along with two representative magnetic field lines. The cooler plasma in the magnetosphere tends to be concentrated in a plasma sheet (not shown) which has roughly the same thickness as the "hot" torus.

be somewhat higher; see Table 1 of *Tariq et al.* [1983]). They found large variations in the particle intensities between 0350 SCET and 1200 SCET, the same period during which the plasma depletions were observed with the PLS instrument (Table 1). However, they find no unique signature in these high-energy ions which correlates with the all of the plasma depletions.

Electron intensities obtained with the LECP experiment also show large fluctuations in this region, although similar fluctuations were reported as also being present elsewhere along the Voyager 2 inbound trajectory [*Armstrong et al.*, 1981]. During this period the LECP instrument was operating in a special "stow mode." As a result, the instrument was primarily sensitive to electrons with energies of 70 keV and above [*Armstrong et al.*, 1981]. A recent reanalysis of the LECP electron data in this region may indicate a better correlation between these data and the PLS depletions than has been reported previously [*Khurana et al.*, 1986]. The increases in electron intensity shown in Figure 5 of *Tariq et al.* [1983] do correlate with depletions 8 and 9 (Table 1) in the PLS data. The electron intensities measured by the LECP instrument may show the best correlation of any of the fields and particles measurements with the PLS observations of the depletions.

This possibility is currently under study (*Khurana*, private communication, 1986).

On the basis of these observations, *Ness et al.* [1979] and *Tariq et al.* [1983] noted that the disturbances could be due to a temporal, magnetospheric disturbance. However, these authors also rejected this hypothesis for various reasons. We believe the disturbances observed near Ganymede were due to temporal changes in the magnetosphere, and the observations in favor of this hypothesis are discussed below.

PLASMA OBSERVATIONS

Motivated by the possibility of deriving vector flow velocities in the vicinity of Ganymede and the suggestion that the plasma depletions were not associated with Ganymede [*Coppi and McNutt*, 1985; *McNutt et al.*, 1985; *J. W. Belcher and P. S. Coppi*, private communication, 1984], we undertook a new analysis of data obtained by the Plasma Science (PLS) experiment during the Voyager 2 encounter with Jupiter. The previous analysis of data in this region was carried out assuming a simplified model of the response function of the PLS instrument. This analysis enables one to obtain one velocity component, density, and thermal speed for the components of

TABLE 1. Times of Depletions

Depletion	Start Time (SCET)	End Time (SCET)
1	0352	0400
2	0436	0441
3	0503	0512
4	0517	0531
5	0539	0550
6	0551	0600
7	0723	0746
8	0838	0854
9	0903	0913
10	0917	0922
11	0932	0941
12	1102	1116
13	1148	1202

enhancements in observed plasma density which occurred on day 189 at ~ 2300 SCET and on day 190 at ~ 0400 are apparently the result of the spacecraft crossing the plasma sheet which wobbles up and down with respect to the spacecraft as Jupiter rotates. Another crossing occurred in the disturbed region centered on ~ 1000 SCET. It may be argued that the spectra acquired between ~ 0800 and ~ 1200 SCET are indeed more prominent than those acquired during the preceding 4 hours. This "asymmetry" in the data with respect to the closest

approach to Ganymede is even more prominent in the spectra acquired with the B and C cups in the main sensor of the PLS experiment. The presence of the plasma sheet may be partially responsible for the enhancements; however, the B and C cups also show clear signatures of the colder plasma intermixed with the depletions during the period from ~ 0400 to ~ 0800 SCET. This suggests that whatever phenomenon caused the depletions is also associated with the relatively cooler and more dense plasma in this region as well.

PLASMA BULK VELOCITIES

Plasma density and temperature can be derived from PLS data given an unambiguous ion signature in any of the four Faraday cups which comprise the experiment, if one can assume that the ion distribution function is well described by a convected, isotropic Maxwellian. As each cup can also be used to find the component of convective velocity normal to the cup in question, it follows that an unambiguous signature in three cups is required to compute the convective velocity vector. Data from several cups can also be used to derive more detailed information about the distribution function, e.g., temperature anisotropies and heat flux. The PLS experiment was designed principally to measure such fluid parameters of the highly supersonic proton and alpha particle components of the solar

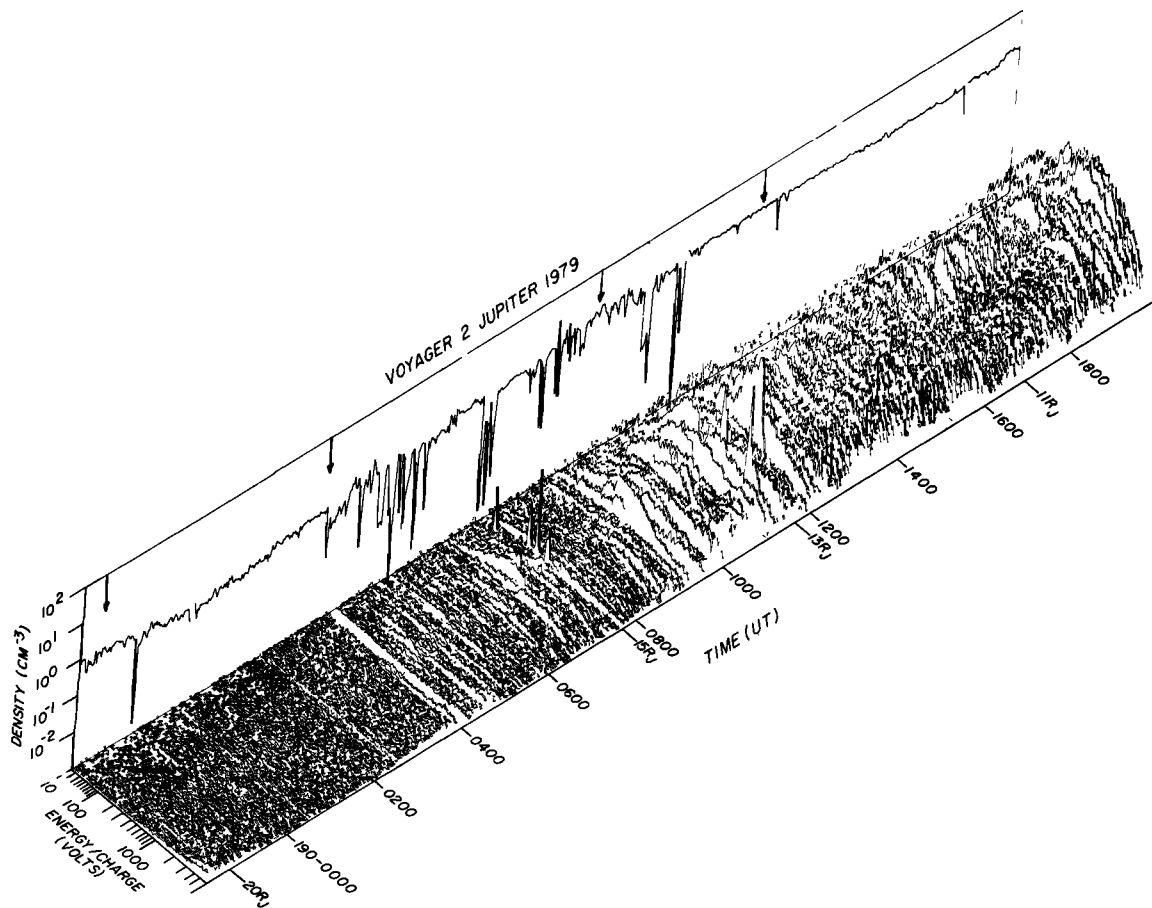


Fig. 2a

Fig. 2. High resolution (M-mode) PLS data taken between day 189 (July 8), 2215 SCET, and day 190 (July 9), 1930 SCET. The detector current (linear scale, 28,000 femtoamperes maximum) is plotted against energy/charge (10 V to 5950 V) and time. The back panel plots an estimate of the total charge density using data from the Faraday cup most nearly pointing into the azimuthal direction at any given time. Figure 2a shows the currents measured in the A cup, Figure 2b those in the B cup, etc.

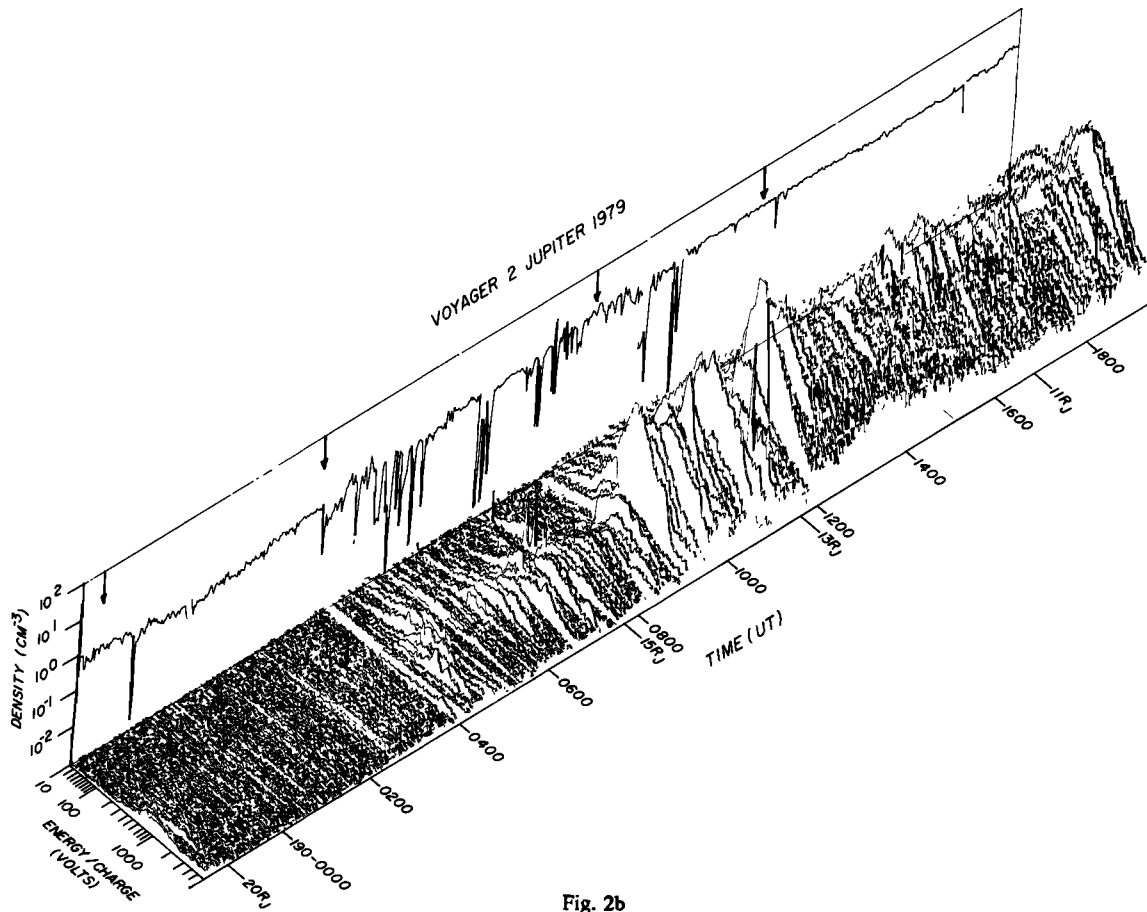


Fig. 2b

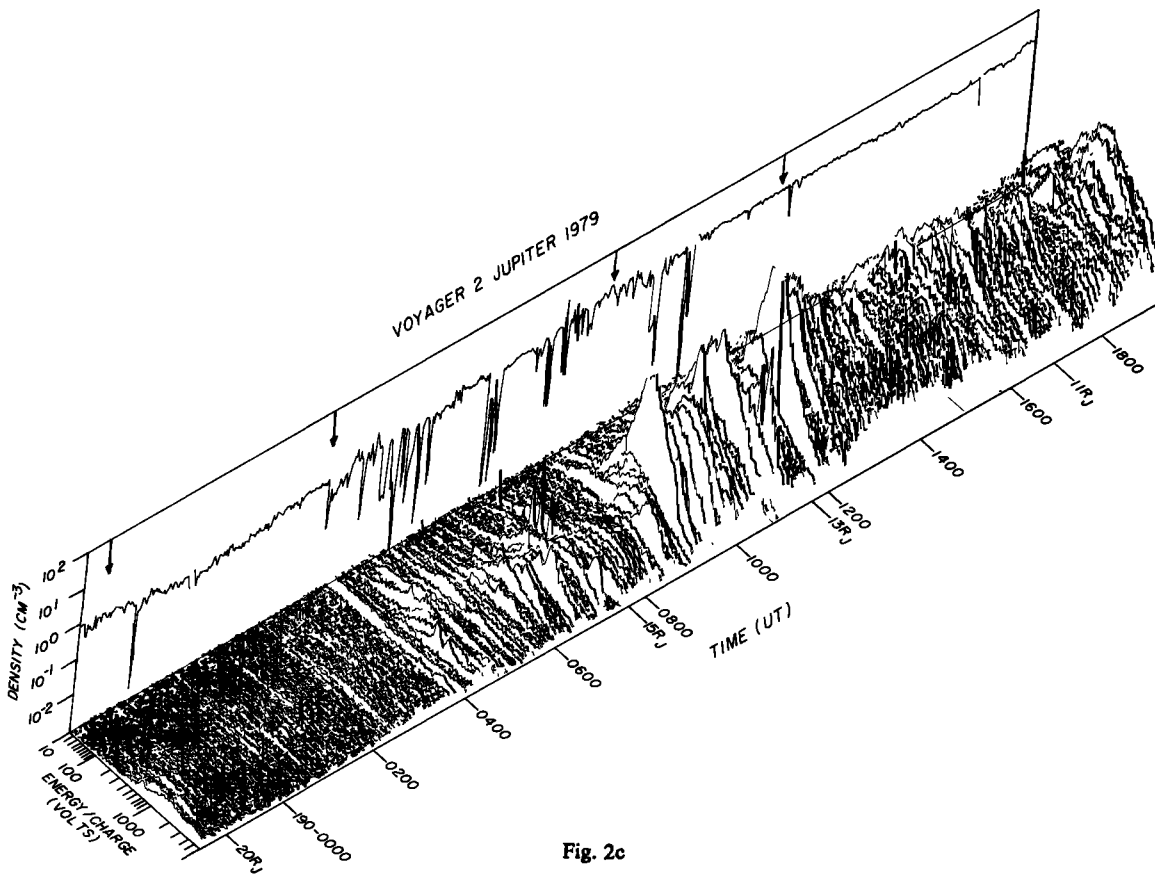


Fig. 2c

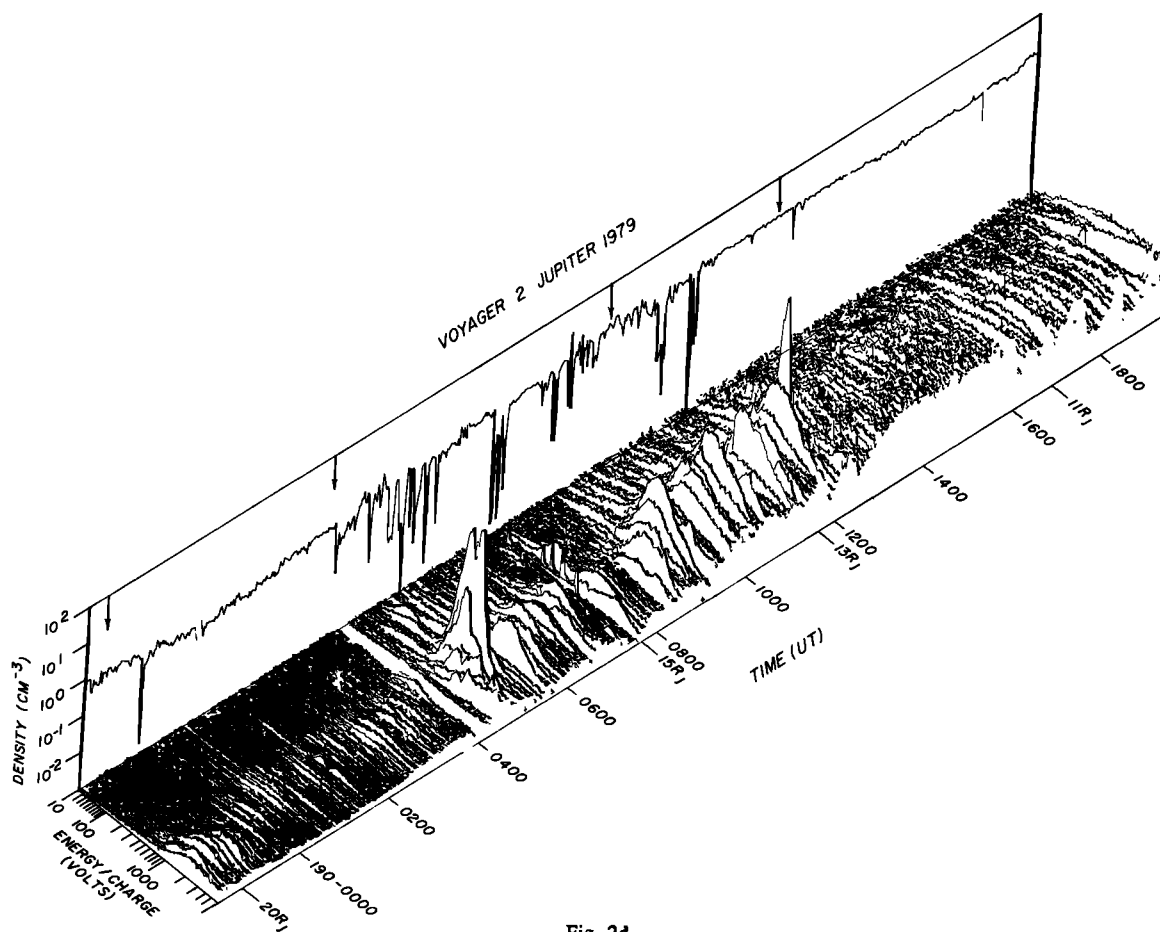


Fig. 2d

wind [Bridge *et al.*, 1977], a task which it accomplishes well (see, e.g., Gazis [1984]). A fourth Faraday cup (the D cup) was included in the experiment package specifically to obtain magnetospheric plasma parameters during the planetary flybys of the Voyager mission. However, the ideal conditions (highly supersonic flow into three of the cups) for deriving such parameters only occurred within a magnetosphere during the passage of the spacecraft through the cold plasma torus of Io [Bagenal and Sullivan, 1981]. During most of the planetary flybys the analysis was limited to the data acquired by the D cup only [McNutt *et al.*, 1981; Lazarus and McNutt, 1983]. More recently, an accurate model of the response function of the PLS instrument has made it possible to extract information from the data acquired by the other three sensors under conditions of subsonic or transonic flow with a high level of confidence in the results [Barnett, 1986]. This model has been used successfully to obtain the density, bulk velocity (magnitude and direction), and (isotropic) temperature of the two ionic species which dominate the magnetosphere of Saturn [Richardson, 1986]. We have applied the same model to the data acquired during the inbound passage of Voyager 2 in Jupiter's magnetosphere to determine whether the observed depletions of plasma in the vicinity of Ganymede could indeed be the convected remnants of a plasma wake.

Unambiguous determination of the convective velocity vector requires clear signatures of identifiable ion peaks in at least three of the sensors. In the Voyager 2 data obtained at Jupiter the heavy ions are almost never resolved (in contradistinction to the inbound Voyager 1 data), and few spectra show a clear

proton signature in the high-resolution mode of the experiment. The low-resolution mode ("L mode") has a signal-to-noise ratio larger than that of the high-resolution mode by a factor of 8 and frequently exhibits a proton signature. The signature of heavy ions is always present when that of protons is, although these ions are never individually resolved. Modeling of these spectra can, however, produce a velocity vector with small formal errors and a high confidence as long as the spacecraft is not significantly charged, which is the case outside of the depletions [McNutt *et al.*, 1981].

The data show that in addition to the depletions, the surrounding plasma is qualitatively different from that encountered prior to ~ 0430 SCET and subsequent to ~ 1200 SCET on day 190. Between the depletions the plasma is relatively dense and cold, showing pronounced peaks from ions with mass-to-charge ratios near 16, e.g., at 0454 SCET. Most of the spectra show ions whose effective Mach numbers (ratio of velocity component normal to a given Faraday cup to thermal speed) are low enough (≤ 6) that the individual heavy ion peaks are not resolved in a majority of the spectra (see Appendix A of McNutt *et al.* [1981]). Two spectra in Figure 2d clearly show peaks at lower mass-to-charge ratios which we identify as signatures of protons. The first spectrum, at 0454 SCET, is associated with the prominent double ion peak in the figure and is consistent with the identification of the heavy ions as S^{3+} and a combination of O^+ and S^{2+} . A lower energy-per-charge peak is also evident in the spectrum acquired at 0720 SCET. In this spectrum the heavy ions are not resolved, so the identification of the low energy peak as protons is less certain than in the

TABLE 2. Plasma Parameters at 0433 SCET

Ion	Density, cm^{-3}	Thermal Speed, km s^{-1}	Temperature, eV
H ⁺	0.666	176	161
S ³⁺	0.369	55.3	510
O ⁺	0.770	65.5	358
O ⁺ hot	1.56	201.6	3390

Alfven speed, 340 km/s; Alfven Mach number, 0.524; Plasma β , 0.195; Bulk velocity, 178 km/s.

spectrum at 0454, but this identification is the most plausible one possible, given the various ionic species which have been identified in the Jovian magnetosphere. Although the exact composition of the magnetospheric plasma cannot be obtained without some assumptions for most of these spectra, the unresolved peak at high energy-per-charge does not vary its maximum in energy-per-charge by an amount qualitatively different from the two spectra we just singled out.

Taking all of these caveats into account, we have used the model of the full response of the PLS instrument to derive values of the plasma properties sampled by Voyager 2. It has not yet been possible to model all of the data contained in the various spectra, i.e., detailed compositional information has not always been extracted. The unresolved peaks complicate the analysis to the extent that a large amount of computational time is required for such a task. Accurate determination of the velocity vector does not necessarily require such extensive analysis (subject to the constraints enumerated above); however, it is desirable to have a good knowledge of the other plasma parameters in this region. With this in mind, we have performed an exhaustive analysis on the L mode spectra obtained at 0433 SCET and obtained the parameters shown in Table 2.

The thermal speeds are high because we have probably not included all of the ion species present in the plasma in the fit. We have modeled the warm ion background with an additional thermal population of O⁺, although this population is almost certainly neither a Maxwellian nor solely composed of oxygen ions. Nonetheless, we have found that such a treatment generally yields good values for the plasma β and plasma mass density when detailed checks of the procedure are possible with resolved spectra.

There are a few cases in which at least one ion peak is clearly resolved, so that the modeling effort required to extract the bulk flow vector is minimal. Even in these cases one must still supply a mass-to-charge ratio to derive the magnitude of the velocity vector. Such extreme cases are shown in Figures 3 and 4 (both high-resolution M mode spectra). In the spectra of Figure 3, two "cold" (i.e., supersonic with respect to the Faraday cups) ions are superimposed on a "warm" (i.e., subsonic) background in three of the four cups. The cold components, indicated by the arrows, have values of mass-to-charge in the ratio of 1.5 to 1. Given the various ionic species which have been identified in the Jovian magnetosphere [McNutt *et al.*, 1981; Bagenal and Sullivan, 1981; Broadfoot *et al.*, 1981; Bagenal, 1985; McNutt, 1982], the most plausible identification of the ions causing these spectral peaks is S³⁺ ($M/Q = 10 \text{ 2/3}$) and O⁺ and S²⁺ ($M/Q = 16$). This identification also yields a "reasonable" value for the magnitude of the velocity vector.

The spectra shown in Figure 4 also display two spectral peaks; however, the most plausible identification in this case is H⁺ for the lower peak in energy-per-charge and a combination of ionic species with larger mass-to-charge ratios for the higher

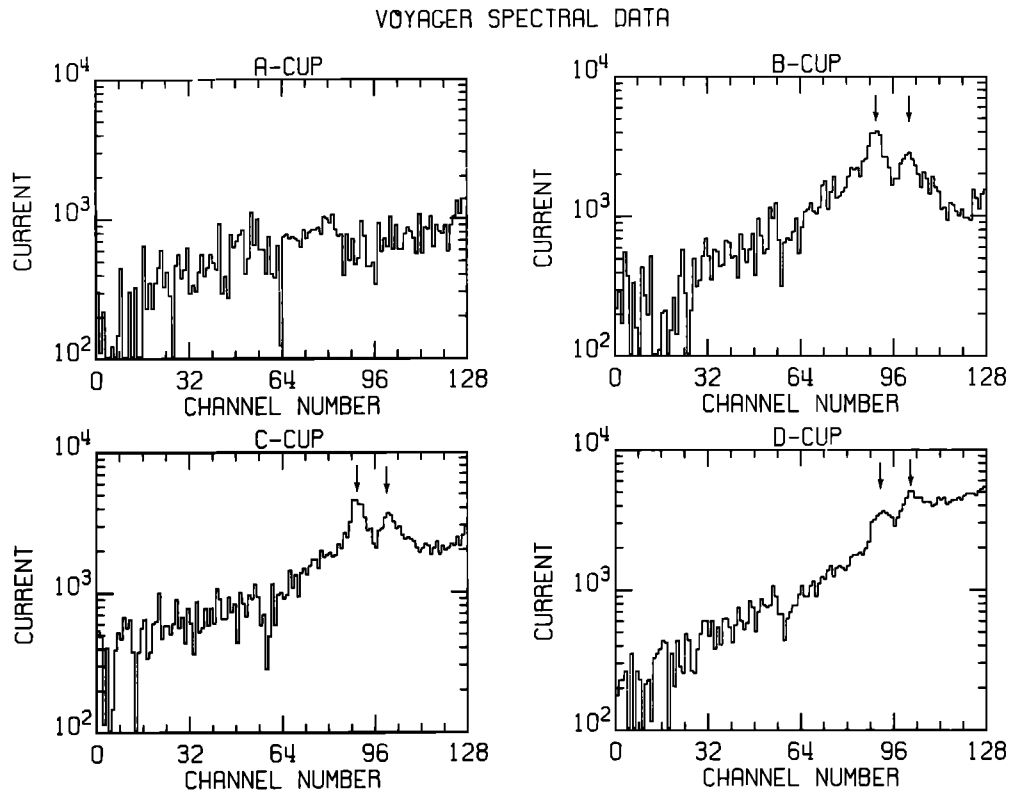
peak. Although two clear spectral peaks appear in the simultaneous spectra from each of the four cups, a good fit to all of the low energy-per-charge peaks in all of the cups cannot be obtained by assuming an isotropic Maxwellian distribution. A good fit to the data was obtained by using a more complex version of the response algorithm which allows for a thermal anisotropy along the local magnetic field. In this case a convected, bimaxwellian distribution yielded a good fit with a ratio $T_{\parallel} / T_{\perp} \sim 3.1$. Similar anisotropies and/or charging of the spacecraft complicate the analysis of some of the spectra which show resolved ion peaks.

In Table 3 we list the times of the spectra which we have been able to model with a high degree of confidence together with the locations of these spectra, referenced to a cylindrical coordinate system (R, z) defined by Jupiter's dipole moment. The derived velocity components are given with respect to a cylindrical system (ρ, ϕ, z) defined by the spin axis of the planet. The numbers in parentheses refer to the values of v_{ϕ} corresponding to rigid corotation with the planet.

The variation in the velocity components is pronounced with v_{ρ} positive from ~ 0430 to ~ 0500 and negative at the other times. The z component (perpendicular to Jupiter's rotational equator) shows a more random variation. It should be noted that the geometrical relationship of the Faraday cups with respect to the primarily azimuthal flow makes them somewhat more sensitive to radial components of plasma flow than to "north-south" components.

The information content of Figure 2 is obviously very much greater than that of the table, but it is difficult to quantify because of the expense and time required to do a full nonlinear least squares analysis on each spectral set. We have attempted to perform a more qualitative analysis as follows. If the plasma flow were very supersonic (effective Mach number ≥ 10) with respect to three of the cups, we could obtain the velocity vector very accurately by assuming that the velocity component into each cup was simply given by the square root of the energy-per-charge value at the peak current of the spectrum divided by the mass per charge of the ion producing the spectrum. This technique can be applied in a very straightforward manner in the solar wind, whose principal ionic component is highly supersonic protons.

The positive ions of the Jovian magnetospheric plasma do not strictly obey these criteria; however, the shape of the high energy, unresolved peak indicates that the plasma flow into the sensor is supersonic and therefore that the energy-per-charge at the maximum of the peak is a good indicator of the bulk flow velocity. The spectra obtained after 1300 SCET show a much broader peak in the spectra obtained simultaneously by all sensors. This indicates subsonic flow from which it is more difficult to extract a convective velocity vector without extensive modeling or a priori knowledge of the plasma composition. Since the flow in the region of interest is transonic to supersonic and the dominant species of the "middle magnetosphere" (≥ 10



JUPITER MAGNETOSPHERE

$B = (-27.274, -21.599, -62.560)$ GAMMA

VOYAGER 2 CHARGE DENSITY ESTIMATE = (1.675)

1979 190 0422:34.086 VCUP = (13.719, 97.415, 114.484, 184.352) KM/S

$R = 16.787$ $\rho(\text{MAGNETIC}) = 16.743$ $Z(\text{MAGNETIC}) = -1.221$ RIGID COROTATION SPEED = 210

Fig. 3. M-mode spectral set measured on day 190 at 0422:34.086 SCET, $16.787 R_J$ from the center of Jupiter in the vicinity of a plasma "dropout." The maxima located by the arrows are probably produced by S^{3+} and O^+ (or S^{2+}), respectively. The signatures in three of the cups allow the determination of all three components of the plasma bulk velocity vector.

R_J) has a mass-to-charge ratio ~ 16 , we can use the algorithm described above to quantify the flow velocity, keeping in mind the possible problems with and limitations of this method.

Figure 5 shows the velocity components derived by applying this technique to the L mode spectra acquired by the B, C, and D cups between 0300 and 1300 SCET on day 190. A mass-to-charge ratio of 16 was assumed for the calculation. If the true mass-to-charge ratio were instead R , all of the velocity values would have to be multiplied by the square root of $16 / R$. Disconnected points and broken lines show the location of spectral sets for which the maximum current was observed in the highest channel of at least two of the cups; in such a case the algorithm used gives totally spurious results, and these are not included here. The velocity components are referenced to an inertial (i.e., nonspinning) reference frame whose z axis is aligned with the spin axis of Jupiter. Cylindrical coordinates (ρ , ϕ , z) are used, as in Table 3. The bottom panel of the figure shows the positive ion charge density computed for the L mode spectra as it was for the M mode spectra in the back panels in Figure 2. The major depletions can be readily identified; the locations of the thirteen canonical ones shown in Figure 1 are indicated by the boxes on the plots of the velocity components. Dotted lines in the velocity component panels indicate the nominal component values for a rotation-dominated magnetosphere: no ρ or z component and a ϕ component

proportional to the distance from the planetary spin axis. The large solid dots show the component values obtained by doing a full nonlinear least squares fit to at least one ion component of a spectrum. The values are those listed in Table 3 which fall within the time period depicted.

In general, the individual nonlinear fits prior to the central depletion region give results which are consistent with the simplified algorithm. The agreement with the last three fits (0742, 0948, 1025 SCET; compare Table 3) is not as good, especially for the ρ component of the velocity. In each of these cases the (presumed) proton peak was used in the fit, as it is the only species which is resolved. There were problems with these fits, made explicit for the fit to the spectrum at 1025 SCET by the two heavy dots. Although a resolved peak appears in spectra acquired simultaneously in each of the four cups, a fit to a convected, isotropic Maxwellian distribution is possible for only three of the cups at a time. This procedure yields the two extreme sets of velocity components which are shown in Table 3 and are plotted in Figure 5. This variation can be taken as the upper limit in the inherent error in the worst of the fits; the formal errors are all much smaller. We have attempted to fit this spectral set with a bimaxwellian distribution but have had no success. This suggests that the spacecraft may have been charged negatively at this time, accelerating the protons into all four cups; however, we have been unable to verify this

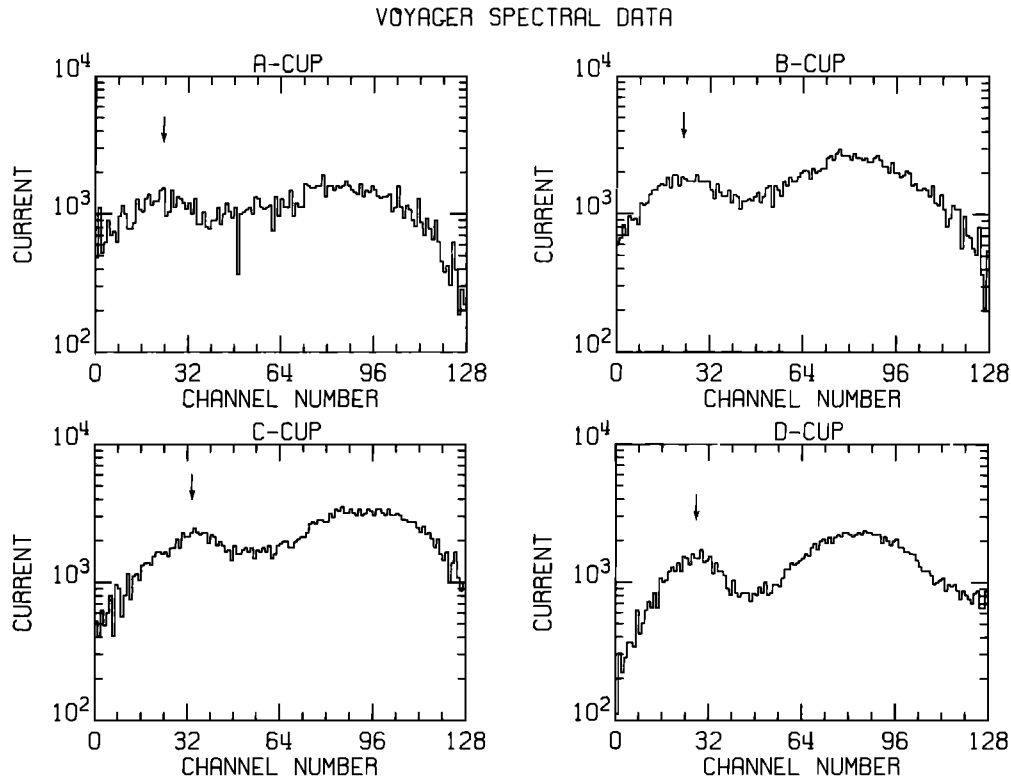


Fig. 4. M-mode spectral set measured on day 190 at 0720:10.078 SCET, 15.177 R_J from the center of Jupiter in the vicinity of a plasma "dropout." The maxima located by the arrows are produced by protons and a combination of heavy ions, respectively. The proton signature can be fit well by a convected, bimaxwellian distribution function.

hypothesis quantitatively. Given these difficulties, the large values of v_p found at 0948 and 1025 (first entry in table) must be treated as suspect; however, they are useful in that they do define hard upper limits.

Although these diverse problems plague detailed analysis of most of the spectra obtained at Jupiter by the PLS experiment on Voyager 2, the rough agreement between the components obtained using the simplified algorithm and those obtained using the detailed analysis shows the following important points. The plasma flow is primarily azimuthal in this region with roughly the magnitude expected for rigid corotation, although tending to be less, especially for the detailed fits, in agreement with previously reported results based solely upon data obtained with the D cup [McNutt et al., 1981]. There is a variation in the z component of flow directly correlated with the location of the spacecraft with respect to the magnetic equator. This correlation indicates flow away from the magnetic equator, a result qualitatively derived previously by other means [Belcher and McNutt, 1980; McNutt et al., 1981].

Using both the algorithm described above and the velocity vectors listed in Table 3, we have computed the velocity components parallel and perpendicular to the measured magnetic field in a coordinate system rotating with the locally measured angular velocity. These values are shown in Table 4.

We find that the bulk motion tends to be parallel to the

magnetic field at the largest southern magnetic latitudes and antiparallel at more northern latitudes. By expressing the velocity data shown in Figure 5 in terms of $v_{||}$ and v_{\perp} , we find that $v_{||}$ changes from negative to positive around 0530 and back to negative around 1100. Hence the field aligned component of the flow appears to be toward the planet and away from a surface warped with respect to the equatorial plane of the magnetic dipole of Jupiter.

The field-aligned component is ~ 50 km/s but varies by as much as an additional 30 km/s. This is a significant speed for plasma to move in the magnetosphere (20 km/s is about $1 R_J/h$). The algorithm, previously referred to, shows the magnitude to be an increasing function of latitude, but the individual components from the fits do not show such a clear picture, half of them exhibiting inflow. The flow component of the fitted spectra perpendicular to the local magnetic field exhibits modest outflow (~ 10 km/s) at higher latitudes ($> 1.5 R_J$ from the magnetic equatorial plane) and larger speeds (up to 100 km/s) at lower latitudes. This trend is not as evident using the components generated by the qualitative algorithm but is still suggested by that technique.

To summarize, the vector flow velocity components have been obtained in the region of the dropouts by using two techniques, each with obvious drawbacks. We have confirmed that the dominant plasma motion is azimuthal but that there is

TABLE 3. Plasma Bulk Velocities

Time (SCET)	R, R_J	z, R_J	Mode	$v_p, \text{km s}^{-1}$	$v_\phi, \text{km s}^{-1}$	$v_z, \text{km s}^{-1}$
0422	16.7	-1.22	M	-65.1	219.7 (210.6)	22.5
0433	16.6	-1.51	L	20.3	176.5 (209.4)	-14.7
0453	16.4	-2.02	L	29.1	150.5 (207.0)	8.41
0454	16.4	-2.04	M	21.3	146.6 (206.9)	-3.34
0719	14.9	-2.93	L	-37.7	151.9 (190.4)	-34.4
0724	14.9	-2.87	L	-24.7	101.0 (189.8)	-19.4
0742	14.7	-2.62	M	-10.78	286.2 (187.8)	1.83
0948	13.9	-0.08	L	-122.3	118.2 (174.2)	-7.53
1025	13.6	0.56	M	-96.7	133.6 (170.3)	1.72
				-2.89	200.5 (170.3)	27.4
1848	10.1	-2.80	M	-16.3	136.9 (130.5)	-13.3

also a significant field-aligned component of flow which modifies somewhat the original estimates of the azimuthal speed (these were based upon assuming the velocity was totally azimuthal [see McNutt *et al.*, 1981]. We have also found evidence of a cross-field flow which may be substantial and planetward in the region of the depletions. Finally, and most importantly in terms of the "Ganymede wake" hypothesis, the nonazimuthal flow is never greater than 150 km/s and is usually a great deal less.

SHORTCOMINGS OF THE "GANYMEDE WAKE" HYPOTHESIS

Ganymede apparently possesses no substantial atmosphere, ionosphere, or intrinsic magnetic field [Wolff and Mendis, 1983], so the interaction of this Galilean satellite with Jupiter's magnetospheric plasma is presumably similar to the interaction of the Moon with the solar wind. The principal effect of Ganymede would be to absorb the magnetospheric plasma overtaking it in its orbit, producing a "wake" leading the moon

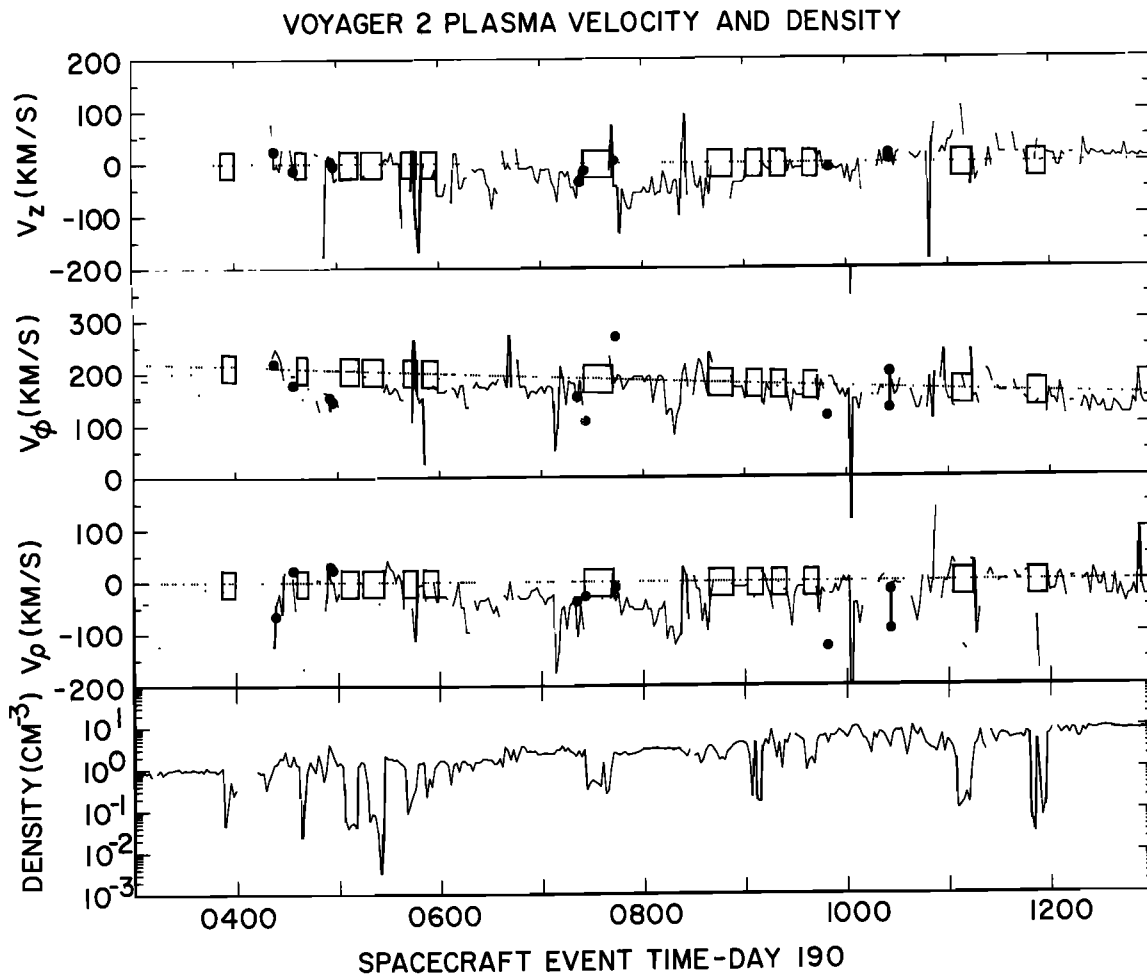


Fig. 5. Plasma parameters on day 190 between 0300 and 1300 SCET. The top three panels show estimates (solid lines) and fits (heavy dots) for the three components of the bulk velocity vector (V_ρ , V_ϕ , V_z) of the magnetospheric plasma. The z axis of the cylindrical coordinate system is aligned with Jupiter's spin axis. The dotted line indicates the values expected for plasma flow rigidly corotating with the planet. The boxes indicate the positions of the plasma depletions as determined from the density estimate for positive ions (lower panel) and for low energy electrons (not shown).

TABLE 4. Plasma Parallel and Perpendicular Velocity Components

Time (SCET)	z, R_J	$v_{\parallel}, \text{km s}^{-1}$	$v_{\perp}, \text{km s}^{-1}$
0422	-1.22	-60.96	-93.76
0433	-1.51	-41.97	-0.12
0453	-2.02	-38.84	8.16
0454	-2.02	-27.47	6.51
0719	-2.93	68.75	13.78
0724	-2.87	42.21	4.79
0742	-2.62	42.14	18.22
0948	0.08	36.33	-121.64
1025	0.56	7.74	-99.48
		2.80	-5.40
1848	-2.80	32.81	8.83

as it orbits Jupiter. Such a phenomenon was anticipated prior to the closest approach of Voyager 2 to Jupiter.

Details of such an interaction have been considered by *Tariq et al.* [1985]. They find that a true wake should have a width of $\sim 2 R_G$. An upper limit for the downstream length of a wake can be obtained by neglecting the self-consistent ambipolar electric field and assuming that the wake fills due to the finite thermal speed of the ions. A typical convection speed for the plasma in this region is between 100 and 150 km/s (Table 3). Thermal speeds range from ~ 170 km/s for protons to ~ 50 km/s for the higher mass ions. This translates into temperatures of \sim a few hundred electron volts (the 40 eV quoted by *Tariq et al.* [1985] is anomalously low in this region; also cf. Figure 12 of *McNutt et al.* [1981]). The sonic Mach number is no more than 3.5, so a wake $2 R_G$ in diameter should be filled in roughly $4 R_G$ downstream. As the closest approach of the spacecraft to the moon was $24 R_G$, Voyager 2 could not have seen a simple geometrical wake (although the follow-on Galileo orbiter probe may be able to do so during one of its gravitational swingbys of the moon).

The radial displacement of the depletions still remains a problem even if some unknown mechanism suppresses the thermal filling of the wake. *Ness et al.* [1979] and *Burlaga et al.* [1980] note that radial motions of the magnetosphere produced by long wavelength Alfvén waves could cause a single depletion structure to appear as a series of depletion regions (the "drapery" model). However, they also note that the spatial locations of the plasma depletions imply that outflow speeds of ~ 500 km/s and inflow speeds of up to ~ 200 km/s are required for such an explanation to hold. Even with the uncertainties in the analysis, such large radial velocities of the plasma in the vicinity of Ganymede can definitely be ruled out. In addition, detailed analysis of the spectra obtained at 0433 SCET (see above) indicates an Alfvén velocity of 340 km/s, whereas the maximum fractional change in the magnetic field is about 0.1 [*Ness et al.*, 1979]. Radial velocity perturbations resulting from Alfvén waves would be, therefore, only ~ 34 km/s, consistent with the magnitude of observed variations but insufficient to explain the locations of the depletions. The drapery model can, therefore, definitely be ruled out as a possible explanation for the depletions.

Tariq et al. [1985] consider the possibilities that the radial spread might be due to the excitation of the Kelvin-Helmholtz instability or to the distortion of the magnetic field geometry by the strong magnetospheric current sheet, an idea due to *Connerney et al.* [1981]. We have shown above that the required radial velocity components do not occur, and *Tariq et al.* [1985] note that the Kelvin-Helmholtz instability might not

be able to produce such large deviations in the plasma flow in any event.

To test the hypothesis that the depletions might still be produced by Ganymede via the "sweeping out" of plasma on flux tubes connected with the moon, we have indicated the spacecraft trajectory, locations of the depletions, and model field lines in a magnetic meridional plane. This is shown in Figure 6 along with arrows indicating the direction of the magnetic field as measured by the spacecraft magnetometer. We have assumed that the symmetry axis of the system is given by the direction of Jupiter's internal dipole moment (a slightly better fit to the magnetic field data was found by *Connerney et al.* [1982] by assuming the "centrifugal equator" for the symmetry surface). The magnetic field lines are labeled by L_{eff} , i.e., the radial distance at which the field line would cross the equator (scaled in planetary radii) if there were no current sheet. This is equivalent to setting the parameter I_0 to zero in the current sheet model [see *Connerney et al.*, 1981]. The field lines themselves were generated with an analytic approximation to the model which is more easily used than the integral expression for the vector potential in the original model (R. L. McNutt, Jr., manuscript in preparation, 1987). We calculated the excursion of Ganymede using the value of I_0 appropriate for the Voyager 2 encounter [*Connerney et al.*, 1981] and found that Ganymede has an excursion over L_{eff} values of 11.56 to 12.15. The first seven depletions occurred at L_{eff} values starting at 12.34, increasing to 12.75, and decreasing to 12.25. The spacecraft and moon were on connecting L shells only between the times of observation of the seventh and eighth depletions. The eighth through thirteenth depletions were observed on the L shells starting at 11.54 and monotonically decreasing to 10.69.

These results contradict those of *Connerney et al.* [1981], who noted a much more dramatic effect due to the field line distortion produced by the current sheet. We found that if the value of I_0 is increased to the value appropriate for the Voyager 1 encounter [*Connerney et al.*, 1981], the values of L_{eff} traversed by Ganymede become 10.37 to 10.98. In this case the spacecraft could have been on field lines swept by Ganymede from 0310 SCET to 0435 SCET, during which interval the first two depletions were seen. The spacecraft would again have been on connecting field lines between 0745 SCET and 0845 SCET, a time interval including the eighth depletion region.

Aside from the question of why Ganymede would not sweep out plasma from all field lines it traversed, if from any, and possible effects of the small toroidal component of the magnetic field, it is clear that the changes in the current sheet strength and/or configuration between the two encounters strongly affects the interval of time during which the spacecraft and Ganymede

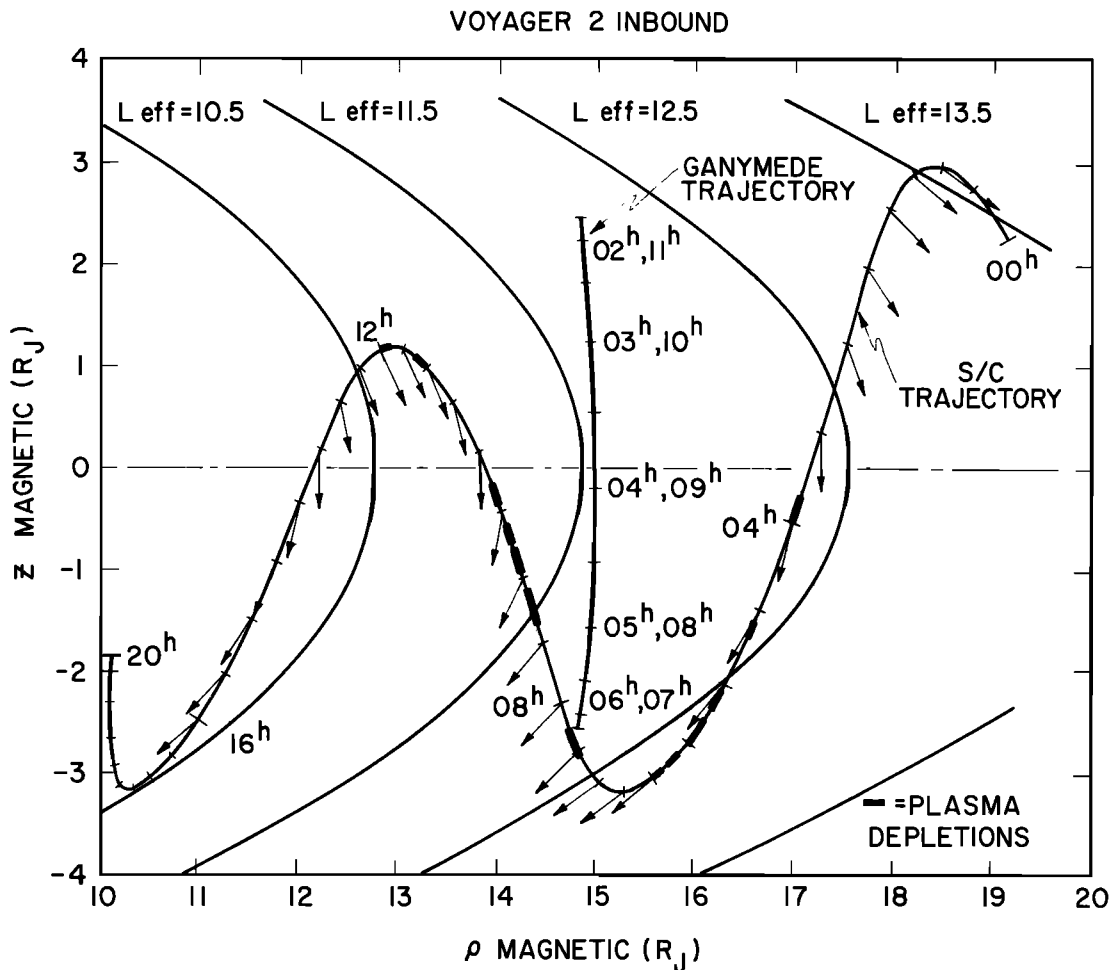


Fig. 6. A "wiggle" plot showing the trajectories of Voyager 2 and Ganymede projected into magnetic meridional planes. The z axis is aligned with the dipole moment of the planet. Arrows indicate the direction of the measured magnetic field, and light lines, the field lines of the CAN model magnetic field appropriate for Voyager 2 [Connerney *et al.*, 1981]. The field lines are obviously distended from those of a vacuum dipole due to the presence of the Jovian current sheet. Large solid dashes locate the plasma depletions along the spacecraft trajectory.

were on the same magnetic field lines. In any case, at most three, and more probably none, of the depletions can be explained by the absorption of plasma by Ganymede. Such a contrived combination of plasma motion and/or diffusion would be required that we must conclude that the plasma voids are not causally linked to the presence of Ganymede; the proximity of the Galilean satellite and the depletions was a coincidence.

"BALLOONING INSTABILITIES" IN THE JOVIAN MAGNETOSPHERE

Having shown that the plasma depletions are not causally related to Ganymede, we suggest that they are manifestations of an MHD instability. In this connection we note that near the equatorial region of the earth's nightside magnetosphere a plasma depletion phenomenon known as the Equatorial Spread F (ESF) is observed [Fejer and Kelley, 1980]. Basu and Coppi [1983] have interpreted this in terms of a gravity driven mode with a characteristic three dimensional structure which locally "unloads" the plasma supported by the magnetic field against the gravitational force. In the case of Jupiter we suggest that a similar process is occurring but in a reversed direction in that here the plasma is "unloaded" outward and away from the

planet. The case of Jupiter also differs from that at the Earth in that (1) the Jovian plasma is characterized by finite values of $\beta \equiv 8\pi\rho/B^2$, whereas $\beta < 1$ in the F layer of the earth's ionosphere and (2) the instability at Jupiter is driven by the combined effects of the plasma pressure gradient and magnetic field curvature, whereas the ESF instability is driven by gravity.

The relevant unstable mode, which can be classified as of the "ballooning" type [Coppi and Rosenbluth, 1966; Coppi *et al.*, 1968; Coppi, 1971; Coppi *et al.*, 1979a] at the edge of the "second stability region" [Coppi *et al.*, 1979b], should produce a double string of plasma depletions ("bubbles") located symmetrically relative to the magnetic equatorial plane. We note that the formation of rising "bubbles" resulting from the onset of gravity-driven interchange modes that obey the frozen-in law has been described by detailed numerical simulations (see Zalesak *et al.* [1982] and references therein) in order to explain the ESF development. In the case of the Jovian magnetosphere the bubbles should develop where the relevant instability is excited with a characteristic double-peak amplitude relative to the equatorial plane. They will then drift toward the planet and manifest themselves as a double sequence of plasma depletions. On this basis, an intermittent plasma-unloading process can be

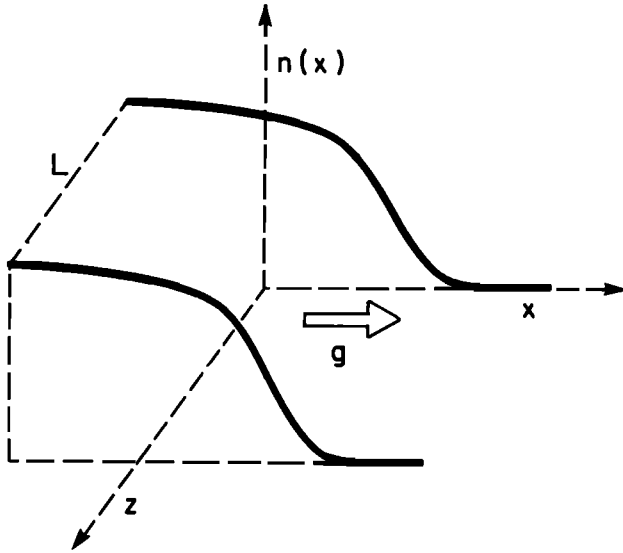


Fig. 7. One-dimensional model configuration of a magnetically confined plasma subject to an effective gravitational acceleration.

envisioned, and we argue that this is a possible explanation of the observed plasma depletions.

Referring to Figure 6, we note that the depletions were indeed detected at both northern and southern magnetic latitudes and that the depletions occurred away from the magnetic equator but not just at the turning points of the spacecraft's latitudinal motion. Therefore, off-equator sightings must be more than just a "dwell" effect (originally the depletions had been recognized as occurring at southern magnetic latitudes, and, after the theoretical model of the structure of the mode was presented, it was realized that depletions occurred at northern latitudes as well). The trajectory of the spacecraft sampled the south magnetic latitudes more, so the predominance of observed depletions below the magnetic equatorial plane resulted from a sampling problem (cf. Figure 6).

There is some limited evidence, which we do not discuss in detail here, that plasma depletions may have been detected outbound around $20 R_J$ by the PLS experiment on Voyager 2 as well. The aspect of the sensor with respect to the plasma flow as well as electrical interference from other spacecraft systems has, however, made this difficult to confirm, and there is no corroborating evidence from the other fields and particles experiments in this case.

THEORETICAL MODEL

One-dimensional Plane Plasma

In order to illustrate the physical processes we wish to discuss, we start by considering a one-dimensional plane plasma which is subject to a gravitational field and is imbedded in a magnetic field as indicated in Figure 7. The equilibrium condition is

$$\nabla p_o = \frac{1}{c} \mathcal{J}_o \times \vec{B}_o + \rho_o \vec{g}_o \quad (1)$$

where $p = nm_i$, n is the ion number density, m_i is the ion mass, and the remaining symbols are of common usage. We define a coordinate system such that $\vec{B}_o = B_o \hat{z}$, $\vec{g}_o = g_o \hat{x}$, and $p_o = p_o(x)$. We consider density perturbations, from this

equilibrium, of the form

$$\tilde{n} = \tilde{n}(x) e^{-i\omega t + ik_x x + ik_y y + ik_z z} \quad (2)$$

where the tildes refer to linearized perturbation quantities. Thus, if we consider these perturbations to be subject to the frozen-in law

$$\tilde{\vec{E}} + \frac{\tilde{\vec{v}}}{c} \times \vec{B}_o = 0 \quad (3)$$

a bending of the magnetic field lines will also be associated with the perturbations as $k_{\parallel} \neq 0$; we expect this effect to counteract the destabilizing effect of gravity. The remaining equations needed to close the set and describe the modes of interest are

$$\rho_o \frac{\partial \tilde{\vec{v}}}{\partial t} = -\nabla \tilde{p} + \frac{1}{c} (\tilde{\mathcal{J}} \times \vec{B}_o + \mathcal{J}_o \times \tilde{\vec{B}}) + \tilde{p} \vec{g}_o$$

$$\frac{\partial \tilde{p}}{\partial t} + \tilde{\vec{v}} \cdot \nabla \rho_o = 0$$

$$\nabla \cdot \tilde{\vec{v}} = 0 \quad \nabla \cdot \tilde{\vec{B}} = 0 \quad (4)$$

$$-\frac{1}{c} \frac{\partial \tilde{\vec{B}}}{\partial t} = \nabla \times \tilde{\vec{E}}$$

$$\tilde{\mathcal{J}} = \frac{c}{4\pi} \nabla \times \tilde{\vec{B}}$$

The condition of incompressibility $\nabla \cdot \tilde{\vec{v}} = 0$ has been introduced to simplify the analysis without losing the essential physical ingredients and replaces the equation of state. We apply the operator $\hat{z} \cdot \nabla \times$ to the momentum equation and then use the other equations in (4) to simplify the result, noting that $k_x \gg (L_x)^{-1}$, where L_x is the scale length for variation in the equilibrium parameters in the x direction (cf. section II of Coppi *et al.* [1979a]). Finally, let $k_x \ll k_y$, so that the velocity perturbation is primarily in the x direction. We obtain the dispersion relation

$$\omega^2 = -g \left| \frac{1}{n_o} \frac{dn_o}{dx} \right| + k_{\parallel}^2 v_A^2 \quad (5)$$

where $v_A^2 = \frac{B^2}{4\pi n m_i}$ and

$$\gamma_{ic} = \sqrt{g \left| \frac{1}{n_o} \frac{dn_o}{dx} \right|} \quad (6)$$

is the growth rate of the well-known interchange instability that is found if $k_{\parallel} = 0$. Notice that g is introduced to simulate the effects of both the magnetic field curvature and its gradient. It is convenient to introduce the dimensionless quantity

$$G = \frac{\gamma_{ic}^2}{k_{\parallel}^2 v_A^2} \quad (7)$$

which measures the importance of the factor driving the instability relative to the restoring effect due to the bending of the magnetic field lines. We note that there is no instability for $G \ll 1$, and the system becomes unstable as G exceeds unity.

Two-Dimensional Plasmas and Ballooning Modes

To model the situation in the Jovian magnetosphere, we consider an axisymmetric equilibrium configuration and density perturbations of the form

$$\tilde{n} = \tilde{n}(l, r_1) e^{-i\omega t + in^0\phi} \quad (8)$$

where ϕ is the angular coordinate about the symmetry axis, l measures the distance along a magnetic field line, r_1 is perpendicular to the magnetic field and lies on a meridian plane, and n^0 is an integer. We take $l=0$ to correspond to the equatorial plane and consider perturbations that vanish for $l = \pm L_o$, L_o being a characteristic distance of variation of γ_{ic}^2 and v_A^2 .

We notice that in this case $B = B(l, r_1)$ and the operator $\vec{B} \cdot \nabla$ that was applied on the perturbation in deriving the dispersion relation (5) becomes $B(l) \partial/\partial l$. In particular, we look for modes localized in the transverse direction around a given magnetic surface and take implicitly $n^0/R \gg |(\partial\tilde{n}/\partial r_1)/\tilde{n}|$. Thus we can ignore the r_1 dependence of the perturbation indicated in (8). We take into account the fact that the magnetic curvature also has a significant dependence on l . Then we retrace all of the steps leading to (5) as indicated by Coppi *et al.* [1979a]. We arrive at a dispersion equation for $\tilde{n}(l)$ that is too complex to treat in its generality; therefore we consider it more appropriate to discuss two simple models of it.

The first model is introduced to illustrate the counterpart of (5) and the type of eigenfunctions that correspond to it, considering regimes where the values of β are such that

$$G \equiv \frac{\gamma_{ico}^2 L_o^2}{v_A^2} \leq 1 \quad (9)$$

where $v_{Ao} = v_A$ ($l=0$). Thus a relevant model dispersion equation is

$$\frac{d^2\tilde{n}}{dl^2} + \left[\omega^2 + G - V(l, G) \right] \tilde{n} = 0 \quad (10)$$

where

$$\hat{l} \equiv \frac{\pi l}{2L_o} \quad \omega^2 \equiv \frac{\omega^2 L_o^2}{v_A^2}$$

and $V(l, G)$ is an effective potential that includes the effects of the spatial variation of $B(l)$ and of the magnetic field curvature. The relevant boundary conditions, since $V(l, G)$ is an even function of \hat{l} , are

$$\tilde{n}(\hat{l} = \pm \frac{\pi}{2}) = 0 \quad \text{and} \quad \frac{d\tilde{n}}{d\hat{l}}(\hat{l} = 0) = 0 \quad (11)$$

Then, if we take

$$V(l, G) = G - \frac{G}{\cosh^2 \sqrt{\frac{G}{2}} \hat{l}} + \sqrt{2G} \tan \hat{l} \tanh \left[\sqrt{\frac{G}{2}} \hat{l} \right] \quad (12)$$

the mode profile is described by

$$\tilde{n} = \tilde{n}_0 \frac{\cos \hat{l}}{\cosh \sqrt{\frac{G}{2}} \hat{l}} \quad (13)$$

and has a characteristic ballooning profile. The corresponding dispersion relation is

$$\omega^2 = 1 - G \quad (14)$$

Note that defining the scale length r_p via

$$-\frac{1}{r_p} \equiv \frac{1}{p_o} \frac{dp_o}{dr_1} \quad (15)$$

and introducing the scale for the gradients in the magnetic field R_o , the effective gravitational force becomes $g_{\text{eff}} = c_s^2 / R_o$, where we have introduced the sound speed c_s ($p_o = c_s^2 \rho_o$). The interchange growth rate is then given by

$$\gamma_{ic}^2 = \frac{g_{\text{eff}}}{r_p} = \frac{c_s^2}{r_p R_o} \quad (16)$$

We observe that in the case just considered,

$$G \approx \frac{p}{nm_i r_p R_o} \times 4\pi n \frac{m_i}{B^2} L_o^2 \approx \frac{\beta L_o^2}{2r_p R_o} \quad (17)$$

Therefore the critical value of β above which (14) predicts the instability to occur scales as

$$\beta \propto \frac{2r_p R_o}{L_o^2} \quad (18)$$

In laboratory experiments on axisymmetric, toroidal plasmas, $L_o \propto R_c$ and $r_p/L_o \propto B_p/B_T$, where B_p is the poloidal magnetic field produced by the plasma current and B_T is the applied toroidal magnetic field, and preliminary observations indicate the presence of a transition between regimes for values of β that scale accordingly.

We notice also that the model potential (12) has no more than pedagogical value to illustrate how the dimensionless parameter G is introduced and the severe limitations of (5). When G is of the order of unity, the dependence of the equilibrium magnetic field on \hat{l} is affected by the plasma pressure. Therefore the use of (5), which implicitly assumes k_{\parallel} to be independent of G , is not appropriate for giving an estimate of how the growth rate of ideal ballooning modes changes with G .

INTERMITTENT AND CONTINUOUS PLASMA UNLOADING PROCESSES

Sequence of Instability Regions

As the pressure gradient and, hence, the dimensionless parameter G increase, the magnetic surfaces tend to crowd against each other, and the gradients of all the characteristic magnetic field parameters increase. We argue that this situation occurs in the dayside magnetosphere as the magnetic field lines tend to move toward the "wall" of the magnetopause established by the ram pressure of the solar wind. The crowding of the magnetic surfaces produces a stabilizing effect as the magnetic tension increases and overcomes the destabilizing effect of the increased pressure gradient. This can be described heuristically by the dispersion relation (5) if we replace k_{\parallel} by $k_{\parallel}^0(1 + \epsilon_0 G)$, where ϵ_0 is a constant and simulates the fact that with increasing G the mode is localized over a shorter distance along the magnetic field lines. Thus a new stability regime can be found for $\epsilon_0 G > 1$; this is the so-called "second-stability region" described by Coppi *et al.* [1979b].

We also observe that as G increases further, the mode amplitude will begin to develop away from the region near $l=0$ where the field line tension is the strongest. In this case the amplitude will exhibit a typical double-peaked profile [Ramos, 1984]. The conditions for which this mode becomes unstable indicate the "upper edge" (in the parameter G) of the second-stability region. We can represent this situation with a model

equation which includes effects expected to be present for $G > 1$. In particular, we look for a mode profile of the form

$$\bar{n} = \bar{n}_0 (1 + \alpha \hat{r}^2) \exp\left[-\sigma \hat{r}^2 / 2\right] \quad (19)$$

where $\sigma = 1 + \epsilon_1 G^2$, $\alpha = \epsilon_2 G^3$, and ϵ_1 and ϵ_2 are small numerical coefficients. The forms of the parameters σ and α are chosen to represent the fact that the scale distance of the mode becomes increasingly dominated by the plasma pressure gradient. The model dispersion equation that we adopt is

$$b(\hat{r}) \frac{d}{d\hat{r}} \left[b(\hat{r}) \frac{d\bar{n}}{d\hat{r}} \right] + \left[(\omega^2 + G) - V(\hat{r}) \right] \bar{n} = 0 \quad (20)$$

where the dependence of the variation of B along the field lines is introduced through the coefficient

$$b(\hat{r}) = \sqrt{1 + \alpha \hat{r}^2} \quad (21)$$

and the effective potential

$$V(\hat{r}) = \hat{r}^2 \left[\sigma (\sigma - 6\alpha) + \alpha \sigma^2 \hat{r}^2 + \frac{2\alpha^2}{1 + \alpha \hat{r}^2} \right] \quad (22)$$

The relevant dispersion relation is

$$\omega^2 = 1 - G + \epsilon_1 G^2 - 2\epsilon_2 G^3 \quad (23)$$

For relative extrema to exist in the curve $\omega^2(G)$, we require $\tau \equiv \epsilon_1^2 / \epsilon_2 > 6$. To have both first- and second-stability regions separated by a region of instability, $\omega^2 = 0$ must also have three real roots. From the general theory of cubic equations, this implies

$$\epsilon_1 < \frac{2}{3} \sqrt{\frac{\tau}{6}} \left[\frac{\tau}{6} - 1 \right]^{3/2} + \frac{\tau}{6} \left[1 - \frac{\tau}{9} \right] \quad (24)$$

and enforces the ordering $\epsilon_2 < \epsilon_1 < 1/3$. For example, $\epsilon_1 = 1/4$ and $\epsilon_2 = 1/144$ yields roots of the dispersion relation (23) given by $G \approx 1.55, 3.63, \text{ and } 12.8$, respectively. These roots separate the various regimes, all of which are present for this choice of parameters.

Given that ϵ_1 and ϵ_2 are considerably smaller than unity, we find that if $G \sim 1$ and the criterion for the "first instability region" is barely met,

$$\bar{n} = \bar{n}_0 \exp\left[-\hat{r}^2 / 2\right] \quad (25)$$

and we have a "single-hump" mode.

If, on the other hand, $G \gg 1$, we obtain

$$\bar{n} = \bar{n}_0 \epsilon_2 G^3 \hat{r}^2 \exp\left[-\epsilon_1 G^2 \hat{r}^2 / 2\right] \quad (26)$$

and we recover the "double-hump" mode.

We propose that the onset and development of "double-hump" ballooning modes of the type described by (26) are responsible for the plasma depletions observed by Voyager 2 in the vicinity of Ganymede. The latitudinal spacing (north and south of the magnetic equatorial plane) reflects the mode topology, while the discreteness of the depletions reflects the intermittent nature of this mode.

Dissipative Modes and Nonlinear Processes

In a plasma in which the effects of finite electrical resistivity (whether caused by collisions or wave-particle interactions) are important, dissipative ballooning modes can be excited. These modes are characterized by the fact that the plasma motion is

decoupled from that of the magnetic field lines. Hence the parameter G is no longer relevant and does not have to reach a threshold value for the excitation of these modes. We suggest that such modes constitute one of the basic plasma processes by which plasma is unloaded from the Jovian magnetosphere. We hypothesize that these modes reflect the nonobservation of plasma depletions during much of the Voyager 2 encounter and all of the Voyager 1 encounter with Jupiter for which plasma data is available.

To illustrate this point, we refer to the one-dimensional plane configuration considered previously and use

$$\vec{E} + \frac{\vec{v}}{c} \times \vec{B}_0 = \eta \vec{J} \quad (27)$$

instead of the frozen-in law (cf. (3)). We also introduce the magnetic diffusion coefficient

$$D_m = \frac{\eta c^2}{4\pi} \quad (28)$$

The perturbed magnetic field \vec{B} is now related to the velocity perturbation by

$$-i\omega \vec{B} = i(k_{\parallel} B_0) \vec{v} - D_m k^2 \vec{B} \quad (29)$$

Then by repeating the same steps that lead to (5) we arrive at the dispersion relation

$$\omega^2 = k_{\parallel}^2 v_A^2 - \gamma_{ic}^2 - \frac{k_{\parallel}^2 v_A^2 D_m k^2}{-i\omega + D_m k^2} \quad (30)$$

and in the limit $|\omega| < D_m k^2$ and $G < 1$ we obtain the growth rate

$$\text{Im } \omega = D_m k^2 G \quad (31)$$

It is meaningful to consider this instability to the extent that its growth rate $\text{Im } \omega > \nu_D$, where ν_D is the rate of density diffusion due to electron-ion collisions. This is, in fact, one of the effective thresholds that has to be considered. We also notice that the mode growth rate is speeded up considerably near the condition for marginal stability of the ideal MHD mode. Specifically, if we consider the case where the plasma pressure gradient dp/dr_{\perp} grows to the point where $G = 1$, according to (30) we obtain, for $\omega > D_m k^2$,

$$\text{Im } \omega = (D_m k^2 \gamma_{ic}^2)^{1/3} \quad (31')$$

This is, evidently, much faster than the growth rate represented by (31).

We notice that, as we envision it, the nonlinear evolution of the ideal MHD ballooning modes leads to extreme stretching and crowding of the magnetic field lines, to the point at which an effective $\eta_{\parallel} J$ becomes important and breaks the frozen-in law. Then the constraint imposed by the frozen-in law is no longer enforced, and the plasma is allowed to burst outward through the magnetic field lines, while the field lines "snap back." We may argue that this is the reason why no special magnetic field signature remains associated with the plasma depletions and that enhancements of the higher energy particle populations, such as those detected with the CRS and LEP experiments, may be left over from the "slipping" event and its corresponding electric field. Thus we envision the mode evolution as starting with the process that unloads the confined plasma when the pressure gradient becomes so strong that the threshold for the second instability region is overcome. After a

sufficient amount of plasma has slipped through the magnetic field lines, the instability turns itself off and a quiet phase lasts until the pressure gradient is rebuilt to the level needed to trigger the instability again. Consequently, the spacing of the observed plasma depletions is related to the rate of plasma transport from the Io torus outward and to the pressure exerted on the magnetosphere by the solar wind.

Finally, we point out that the suggestion that ideal MHD ballooning modes driven by the centrifugal force to which Jupiter's magnetospheric plasma is subjected was made by Hasegawa [1980] on the basis of the model equation (5) following the derivation of Coppi *et al.* [1979a]. However, since the onset of ideal MHD ballooning modes corresponds to $G \geq 1$, where the validity of the assumptions underlying the derivation of this model dispersion relation fails, the supporting analysis could not be considered adequate.

COMPARISON OF THE THEORY WITH THE OBSERVATIONS

General Comments

The observations made by the Voyager spacecraft [Krimigis *et al.*, 1981; McNutt *et al.*, 1981] show that there are at least two distinctly different quasi-thermal plasma populations in the Jovian magnetosphere. The "cold" ($T < 1$ keV) ions are responsible for most of the mass in the magnetosphere, while the "hot" ($T > 10$ keV) ions are responsible for most of the pressure. Further analysis has shown that these populations both contribute to the observed current sheet that is the region of our present interest.

The mean kinetic energy of the cold ions is dominated by their corotation velocity v_c as they $\mathbf{E} \times \mathbf{B}$ drift azimuthally about the planet. The relevant acceleration is then

$$g_{\text{eff, COLD}} \approx \frac{v_c^2}{r}$$

where r is the distance from the planet. In the region close to the magnetic equator which we consider ($\Delta z \approx 2 R_J$), most of the contribution to the Alfvén velocity is due to the cold ions and $M_A = v_c / v_A \sim 1$ [McNutt, 1983; McNutt, 1984].

The hot ion population has a pressure p_H corresponding to $\beta_H \sim 1$. The corresponding acceleration is

$$g_{\text{eff, HOT}} \approx \frac{v_{th, \text{HOT}}^2}{R_c}$$

In principle, we must also consider the contribution of the streaming velocity of the cold ions along the magnetic field lines. However, this contribution is less than the thermal speed of the hot ions along the magnetic field [Sands, 1984] and so can be ignored in estimating $g_{\text{eff, HOT}}$.

We notice that $R_c \ll r$ and the scales for the hot and cold plasma pressure and density gradients are comparable, i.e., $r_{n, \text{COLD}} \approx r_{p, \text{HOT}}$ (cf. (15)), so $g_{\text{eff, HOT}} > g_{\text{eff, COLD}}$. Hence, in estimating G we use the acceleration seen by the hot ion population and the Alfvén speed as determined by the cold ion population to obtain (cf. (17)):

$$G \approx \left[\frac{v_{th, \text{HOT}}}{v_A} \right]^2 \frac{1}{R_c r_{p, \text{HOT}}} L_o^2 \quad (32)$$

We notice that at higher latitudes than those we consider, the cold ion population is negligible, while the hot plasma pressure can be considered constant along magnetic field lines. In this

case the Alfvén velocity is to be reevaluated, taking into account that only the hot ion density contributes to it. Hence the characteristic values of v_A would be higher than those considered here.

The Voyager 1 Encounter

We can illustrate the values of and variation in G by calculating some of the relevant plasma quantities obtained during the flybys of the planet. Barbosa *et al.* [1979] determined that the total plasma pressure sampled outbound from $\sim 20 R_J$ to $80 R_J$ varied as $r^{-3.54}$. Their analysis made use of the fact that the spacecraft traversed the magnetic equator twice every planetary rotation period due to the tilt of the magnetic axis of the planet with respect to the rotational axis. There are fewer crossings of the magnetic equator on the dayside of the planet due to the asymmetry of the magnetosphere produced by the solar wind, but we can obtain some information about the pressure and density gradients from the PLS and LECP data sets. On Voyager 1 inbound the charge density at the plasma sheet maxima between $10 R_J$ and $\sim 35 R_J$ varies as $r^{-3.7}$. The composition in the plasma sheet does not show a substantial change, so this gradient is representative of the mass density gradient as well [McNutt *et al.*, 1981]. Just outside of $40 R_J$, the densities are higher than predicted by this trend, suggesting some perturbation to the system. The temperature of the cold component decreases by a factor of ~ 2 or 3 in this same radial range inside the plasma sheet, although the surrounding plasma shows a slight increase in temperature with distance from the planet.

We have found that a power law also gives a good representation of the pressure decrease with distance found in the hot plasma detected by the LECP experiment. Using the data of Figure 24 of Krimigis *et al.* [1981], we find a pressure variation which goes as $r^{-2.5}$ where we have assumed that the local maxima in p are indicative of crossings of the magnetic equator. If we include crossings further out, the exponent changes from 2.5 to 3.0 but remains roughly consistent with the gradient found in the cold plasma density. B. H. Mauk *et al.* (unpublished manuscript, 1985) have recently reanalyzed the LECP data between $9.6 R_J$ and $42 R_J$ for Voyager 1 inbound and found that a good fit to the pressure profile is given by $r^{-\gamma}$, where γ is 3.43, 3.51, or 3.71 depending upon whether the predominant ion is H^+ , O^{+} , or S^{+} , respectively.

We can use (32) to estimate G in the plasma sheet during the inbound passage of Voyager 1 in the vicinity of Ganymede's orbit by taking $M_A^2 = 3$ [McNutt, 1984], $r = 15 R_J$, and $v_{th, \text{HOT}} = 600$ km/s (O^+ ions at 30 keV). The radii of curvature of the field lines differ greatly from those deduced from a dipolar field as a result of the current sheet. At $15 R_J$ a typical value of R_c is $\sim 1 R_J$ (from the model of Connerney *et al.* [1981]) and a typical Alfvén speed is 120 km/s. Using $r / r_{n, \text{COLD}} = 3.7$ and $r / r_{p, \text{HOT}} = 2.5$ (cf. (15)), we obtain $G \sim 4.2 L_o^2 L_c$ in units of R_J , with most of the contribution coming from the hot plasma as a result of the small radius of curvature of the field lines. If the true radius of curvature is larger, then the corresponding value of G will be smaller. Away from the plasma sheet the hot ions dominate both the mass and pressure. In this region we can use (17) to estimate a "local" value of G away from the magnetic equator. Using $\beta \sim 5$ (cf. Figure 24 of Krimigis *et al.* [1981] and discussion by McNutt [1983, 1984] concerning the uncertainty in this number) and values introduced previously for the other quantities, we find $G \sim 0.41 L_o^2$ (this is an upper limit

because the radius of curvature of the field lines is larger in this region). This decrease by an order of magnitude is due to the change in the Alfvén speed with location along a given field line which, in turn, results from the equatorial confinement of the cold plasma. The variation in these estimates of G implies that perturbations will tend to grow most rapidly in the high-density region with values of $L_o \approx 2R_J$ or so, corresponding to a localized ballooning mode rather than the global interchange mode which has usually been invoked (see, e.g., Cheng [1985], Siscoe and Summers [1981], and Summers and Siscoe [1985] and references therein). We emphasize that L_o is the characteristic scale length for the mode at small values of G , whereas the observations refer to the equilibrium corresponding to $G \gg 1$. Hence, L_o is not well known but is at least the "thickness" of the current sheet as measured along the magnetic field lines in the region of interest.

The Voyager 2 Encounter

The Voyager 2 inbound pass, which is of primary interest here, is different in several qualitative respects from the Voyager 1 pass, as has been remarked upon before [McNutt *et al.*, 1981]. The most striking difference is in the thermal structure of the cold plasma, i.e., the well-defined, plasma sheet crossings observed inbound by Voyager 1 are not present in the PLS data set from the Voyager 2 encounter, although the plasma temperature away from the sheet crossings is comparable (~ 100 eV). In addition, we have found that the cross-field pressure and density gradients are different from those found during the inbound part of the Voyager 1 encounter. We believe this difference to be linked intimately to the appearance of the plasma depletions observed by Voyager 2, as we discuss below.

Both the charge density and mass density obtained with PLS show a break in logarithmic slope at about $18 R_J$ [McNutt, 1980]. Some of this effect in the charge density curve may be due to part of the plasma signal being outside of the energy-per-charge range of the detector; nevertheless, some change in slope is present. Near the planet we find the density varying as $r^{-3.8}$; outside of $18 R_J$ the slope decreases, and the density varies as $r^{-1.8}$.

From Figure 26 of Krimigis *et al.* [1981], we find a similar break in the hot plasma pressure detected with the LECP experiment, if we consider only those relative maxima in the pressure between 13 and $19 R_J$ separately from both those further out and the maximum which occurred near closest approach to the planet. A linear regression analysis shows that between $13 R_J$ and $19 R_J$ the hot plasma pressure varies as $r^{-2.5}$; the variation changes to $r^{-3.7}$ between $23 R_J$ and $43 R_J$ on the inbound pass, so there is a change consistent with that seen in the cold plasma population. Outbound from $10 R_J$ to $24 R_J$ the pressure decreases as $r^{-4.9}$ and is indicative of a recovery to a configuration like that seen earlier on Voyager 2 and on Voyager 1 inbound.

In the large gradient region, we find G near the equator to be (using the parameters in Table 2 and (32)) $7.2 L_o^2$ and G away from the equator to be (using (17)) $0.63 L_o^2$ assuming $\beta \sim 2$ [see McNutt, 1984] at $15 R_J$. In the outer region where the slope is less, we have fewer analyzed cold spectra from which we can obtain an accurate value of the Alfvén speed. Near $21 R_J$ we have been able to extract Alfvén speeds and flow speeds from a few spectra. With a bulk speed of ~ 250 km/s, an Alfvén speed of ~ 350 km/s, β of the hot component ~ 2.3 , and a thermal

speed of 600 km/s for the hot (oxygen) ions, we find G to be $0.55 L_o^2$ and $0.21 L_o^2$ near and away from the equator, respectively. This variation suggests that the perturbation scale lengths were also set by the distribution of cold plasma during the Voyager 2 encounter with Jupiter even though the variation in this distribution is less pronounced than that sampled by Voyager 1. This being the case, the pronounced change in the spatial gradients of the particle distribution, which occurred near $18 R_J$, would take the system from a stable configuration to an unstable one, exciting ballooning-type instabilities in the process.

In the Jovian magnetosphere, we expect that if ballooning modes can be excited due to the destabilizing effect of the cold plasma sheet, then large pressure gradients should also lead to a second instability region for the magnetosphere as the flux surfaces are crowded together on the dayside of the planet. For $L_o \sim 1.3 R_J$ the magnetosphere seen by Voyager 2 would become unstable to such modes very near the time the plasma depletions were first observed. Referring to Figure 6, we can see the zeroth order similarity between the spatial structure of the relevant mode and the locations of the depletions.

We note that the values of G / L_o^2 deduced for the equatorial regions of the magnetosphere differ by less than a factor of 2 between the Voyager 1 encounter and the region of large pressure gradients sampled by Voyager 2. We emphasize that only this ratio G / L_o^2 can be estimated reliably; there is much more uncertainty in the appropriate value of L_o . In addition, we note that the value of L_o appropriate for calculating G may have been smaller for the Voyager 1 encounter due to the more rapid variation of Alfvén speed along the field lines in the region of the plasma sheet.

We suggest that the cold plasma population present during the Voyager 1 encounter may have been responsible for (1) changing the instability threshold and (2) leading to dissipative modes via the introduction of an effective resistivity associated with microinstabilities and the lower plasma temperature. The possible importance of such microinstabilities for cross-field transport has been noted recently by Abe and Nishida [1986]. The regions in which plasma depletions were not observed could result from either small values of G and/or the presence of an effective resistivity in the plasma. A more detailed discussion of these possibilities is beyond the scope of this preliminary investigation.

ORIGIN OF CHANGES IN THE PRESSURE GRADIENT

Compressibility of the Magnetosphere

To fully explain the absence of the plasma depletions during most of the Voyager 2 encounter and the Voyager 1 encounter, a mechanism for producing the changes in the cross-field pressure gradient of the confined plasma had to be found. On the dayside of the planet, where the phenomenon was observed, the magnetosphere is confined by the solar wind. The high β plasma within the magnetosphere results in the exact pressure balance surface (the magnetopause) being determined in a very nonlinear but self-consistent fashion. It has been known for some time that the compressibility and large spatial variations of the dayside Jovian magnetosphere are governed by the interplay of the high β magnetospheric plasma and the order-of-magnitude variations in solar wind ram pressure at the orbit of Jupiter [Smith *et al.*, 1978; Slavin *et al.*, 1985]. Theoretical treatments of plasma flow in the magnetosphere have typically

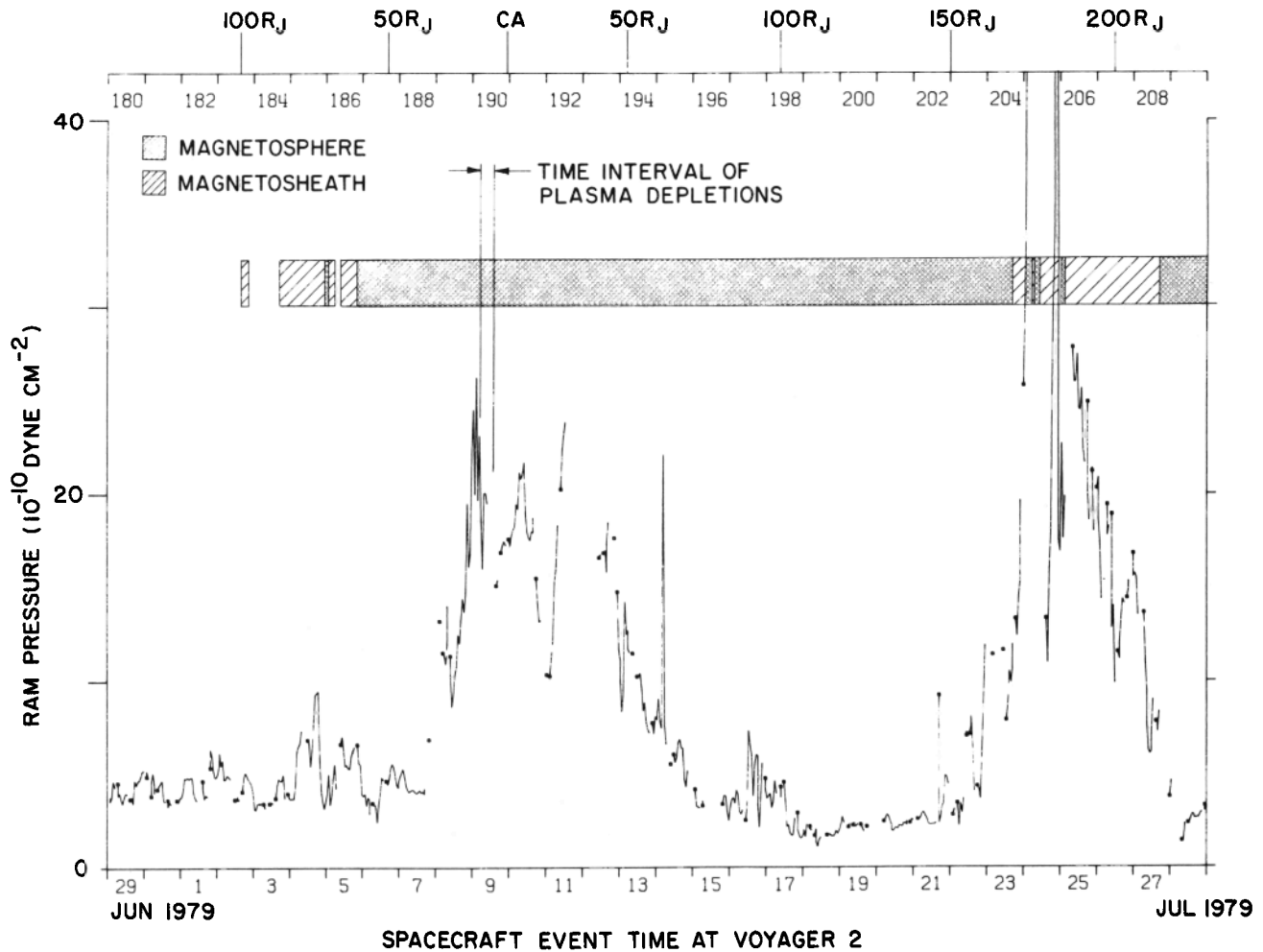


Fig. 8. Solar wind ram pressure at Voyager 2 found from extrapolating the wind parameters as measured downstream at Voyager 1. The pressure is given in units of 10^{-10} dyne cm^{-2} . Distance of the Voyager 2 from the center of Jupiter is indicated at the top (CA denotes the closest approach of the spacecraft to the planet). The crosshatching indicates times during which data taken by Voyager 2 indicated the presence of magnetosheath plasma; stippling indicates the times during which magnetospheric plasma was detected. The time interval during which the plasma depletions were detected (cf. Fig. 5) is also indicated. Times of the boundary crossings are from *Bridge et al.* [1979b].

ignored the weak effects, if any, of the solar wind deep inside the Jovian magnetosphere (see, e.g., *Vasyliunas* [1983]), although it has been recognized that the solar wind induced day-night asymmetry does have important effects [*Hill et al.*, 1983]. There is evidence of some solar wind control as close to the planet as $\sim 10 R_J$ [*Belcher and McNutt*, 1980; *McNutt et al.*, 1981], although it has only recently become possible to evaluate quantitatively this effect [*Sands*, 1984].

We have reexamined the solar wind ram pressure as observed at Voyager 1 and propagated backward in time to Voyager 2 (Figure 8), and as observed at Voyager 2 and propagated forward to Voyager 1 (Figure 9). Both figures show the well-documented correlation between changes in the solar wind ram pressure and crossings of the planetary bow shock and magnetopause. However, they also show that just prior to the time the plasma depletions were observed by Voyager 2 there was an abrupt, large increase in the solar wind ram pressure. The propagation of the solar wind makes no allowance for either the presence of the magnetosphere or the evolution of the solar wind. Using the measured solar wind speed, the travel time of the solar wind between spacecraft during the intervals of

interest is about 40 hours. Making allowance for the timing uncertainties, we conjecture that this rise triggered a rapid compression of the magnetosphere. This accounts for the increased pressure gradient, which reflects the magnetosphere trying to readjust to the changed boundary conditions. At the last inbound crossing of the magnetopause by Voyager 2 the spacecraft was $62 R_J$ from Jupiter, and the solar wind ram pressure was 6.7×10^{-10} dyne cm^{-2} . *Slavin et al.* [1985] find that the distance to the stagnation point at Jupiter scales as the ram pressure of the solar wind to the $-1/4$ power. Using this relation, we find that at the peak pressure on day 190 (Figure 8) of 26×10^{-10} dyne cm^{-2} the standoff distance would have decreased to $44 R_J$. Both this pressure and standoff distance are in agreement with those found by Voyager 1 at its last inbound magnetopause crossing, which occurred at $47 R_J$.

If we assume that the compression of the magnetosphere takes place quasi-statically and that the scaling of *Slavin et al.* [1985] holds, we find

$$v_{r,MP} = -\frac{r_{MP}}{4} \frac{1}{p} \frac{dp}{dt} \quad (33)$$

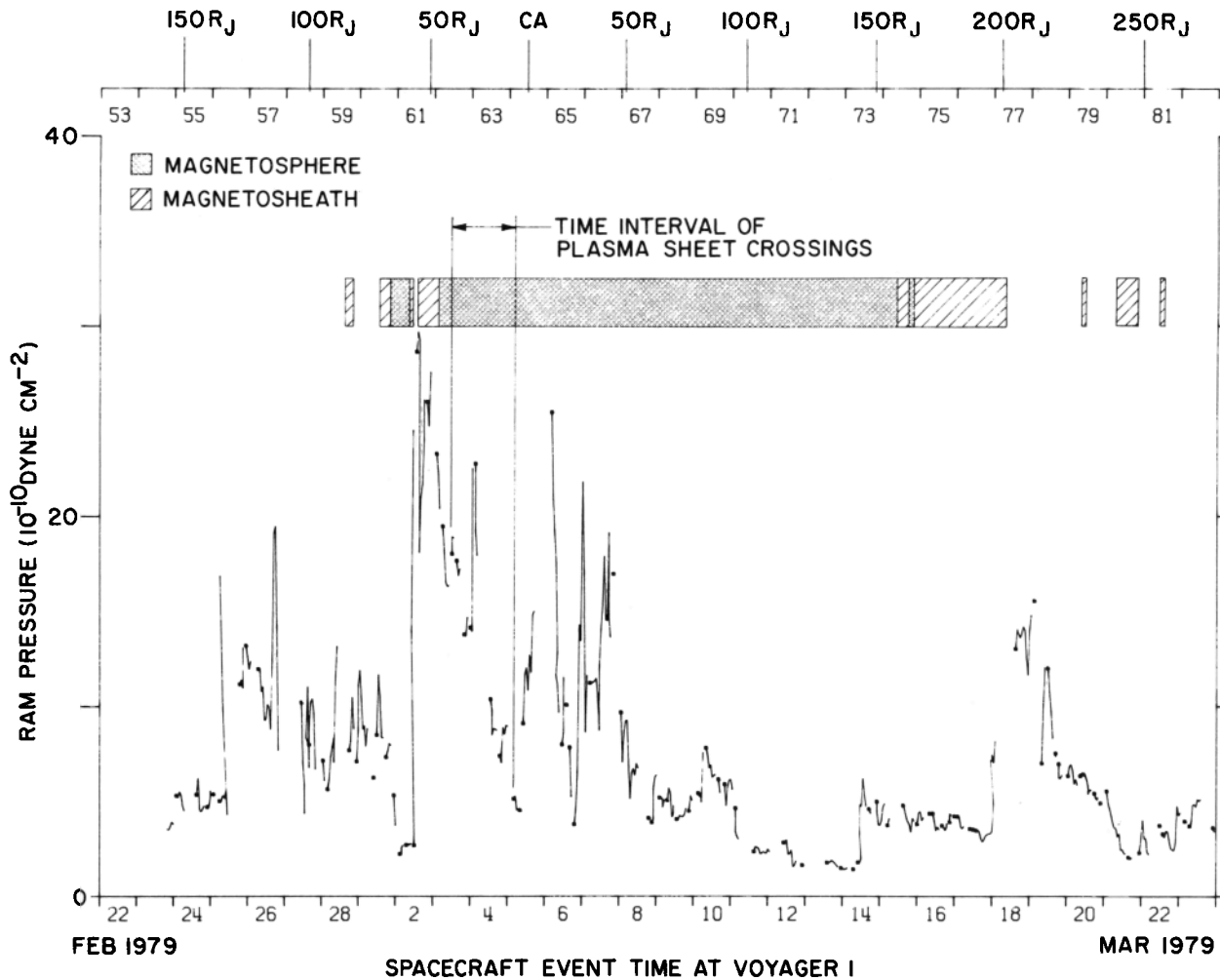


Fig. 9. Same as Figure 8 for ram pressure extrapolated to Voyager 1 from measurements made upstream by Voyager 2. The boundary crossings are from *Bridge et al.* [1979a] with the exception of two crossings of the bow shock on day 80 at 0737 SCET and 2106 SCET (which occurred in a data gap not filled at the time of that publication).

for the radial component of velocity at r_{MP} , the distance to the magnetopause.

We can estimate an upper limit for the radial velocity inside of the magnetosphere by assuming a spherical geometry and that the divergence of the mass flux is zero. Using $\rho \propto r^{-1.8}$ (see above), we find that the product $v_r r^{0.2}$ is a constant inward to $18 R_J$, where the pressure gradient and density gradient steepen. Combining this with (33), we can estimate the local radial velocity component.

The increase in ram pressure took place in about 17 hours, although there is a lot of fine-scale structure which may have been modified by propagation through the solar wind and Jovian magnetosphere in going from Voyager 1 to Voyager 2. Near the peak of the pressure pulse, we find from Figure 8 that $(\frac{1}{p} \frac{dp}{dt})^{-1} \approx 13$ hr. With the magnetopause at $44 R_J$ this gives an inward speed of 17 km/s for the magnetopause. Most of the ram pressure variation results from a region of increased plasma density being convected past the spacecraft at the solar wind velocity, although part of the variation is due to changes in the velocity as well. Allowing for all of these effects, the variation in ram pressure, as propagated to the spacecraft, should be approximately that experienced by the magnetopause. Mass conservation gives an inward velocity of ~ 20 km/s at 18

R_J , where the mass density gradient begins to steepen. A further extrapolation inward to $15 R_J$ yields 5.8 km/s as a result of the larger mass density gradient. In other words, as the gradients increase, the transport velocity decreases. A better treatment of these effects will require a better magnetospheric model; however, these inferred speeds are of the order of magnitude of the nonazimuthal velocity components found in our analysis, so there are no inconsistencies with the compression picture.

Plasma Flow During the Voyager 1 Flyby

To check further the consistency of the compression hypothesis, we have attempted to extract information on the radial component of plasma flow velocity inside of the magnetosphere during the Voyager 1 flyby inbound to the planet. Figure 9 shows a rapid increase in solar wind ram pressure just prior to the entry of Voyager 1 into the magnetosphere at $47 R_J$. The propagation of ram pressure from Voyager 2 shows that this was followed by a decrease almost up to the time of the closest approach of Voyager 1 to the planet at $4.9 R_J$. During the period that the PLS instrument detected the cold plasma sheet (from day 62 1000 SCET, $42 R_J$ from the planet, to day 64 0200 SCET, $11 R_J$ from the planet

[see *McNutt et al.*, 1981]), we find that $(\frac{1}{\rho} \frac{d\rho}{dt})^{-1}$ varied from 62 h to 14 h as propagated to Voyager 1. The corresponding magnetopause standoff distances are $50 R_J$ and $72 R_J$, and outward magnetopause speeds are 4.0 and 25 km s^{-1} , respectively. The mass density varies as $r^{-3.7}$ (see above), so mass conservation yields outflow speeds at the spacecraft which vary from 3.0 km s^{-1} at $42 R_J$ to 1.0 km s^{-1} at $11 R_J$.

These estimates are based upon the constancy of mass within the magnetosphere; however, I_0 is injecting about 1000 kg of newly ionized plasma per second into the system. In a steady state this already implies a radial outflow of the order of 20 km s^{-1} in an axially symmetric disk a few R_J thick [*McNutt et al.*, 1981; *Hairston and Hill*, 1985]. Hence this additional outflow will tend to increase our estimates of the net outflow velocity.

We have recently obtained bulk velocity vectors from many of the Voyager 1 spectra obtained between $11 R_J$ and $25 R_J$ (M. R. Sands, private communication, 1985). As during the Voyager 2 encounter, most of the non-azimuthal flow is field aligned and toward Jupiter. The cross-field component varies but is consistent with outflow in part of this region. We conclude that the Voyager 1 PLS data set is consistent with plasma outflow, indicative of plasma escape via the dayside, an expanding magnetosphere, or both. Details of the flow variations will be addressed in a future publication.

In the colder plasma present in the expanding magnetosphere sampled by Voyager 1, we expect sufficient resistivity (collisional or otherwise) may be present to allow this outflow to occur in addition to that due to the expansion. In fact, associated with the cold positive ions encountered in the plasma sheet by Voyager 1 are cold electrons at temperatures at least a factor of 2 less than seen by Voyager 2. This difference in the electron population alone can account for an increased plasma resistivity during the Voyager 1 flyby which may be of sufficient magnitude to violate locally the frozen-in flux law. Although we have no direct evidence at this time which conclusively points to the presence of cross-field transport via the dissipative modes, many of the requirements for such transport are clearly present during the Voyager 1 encounter. There are no inconsistencies with this transport hypothesis, but, clearly, further analysis of the problem is needed.

Finally, we note that outflow will tend to reduce the azimuthal velocity of the plasma about the planet by simple conservation of angular momentum, but the relatively gentle outflow required by the expansion cannot account for all of the deviation from rigid corotation which is observed [*McNutt et al.*, 1981]. The accepted explanation [*Hill*, 1979] of the deviation in terms of mass loading must still be accepted as valid. In addition, we note that the deviation encountered by Voyager 2 is still present but decreased somewhat in magnitude if allowance is made for the nonazimuthal flow which tends to decrease the component of velocity into the side sensor of the PLS instrument.

Other Differences Between the Encounters

Indirect corroborating evidence of an expanded magnetosphere encountered by Voyager 1 versus a compressed magnetosphere encountered by Voyager 2 is given by the magnetic field data and the temperature of the cold plasma component. *Connerney et al.* [1981] found that the magnetosphere encountered by Voyager 2 was less inflated than that encountered by Voyager 1 (and Pioneer 10). This is reflected in their models by the strength of the current sheet

parameter I_0 , the value of which for the Voyager 2 field model is two thirds that for the Voyager 1 field model. Rather than viewing the "inflation" as some intrinsic magnetospheric property, we note that compression of a flux conserving magnetosphere will increase the magnetic field at a given distance from the planet, leading to a natural explanation of the decreased current sheet present during the Voyager 2 encounter. The external pressure was decreasing as Pioneer 10 approached its closest distance from Jupiter [*Smith et al.*, 1978], so the external conditions were similar to those during the Voyager 1 encounter and qualitatively account for the similarities in the magnetic field data.

Conservation of the first adiabatic invariant implies that the plasma in a compressed magnetosphere will be hotter than that in an expanded one. *Smith et al.* [1978] noted that during the Pioneer 10 encounter, the particle intensity tended to increase when the magnetosphere was compressed. However, there was no evidence for betatron acceleration of the high-energy particles. *Krimigis et al.* [1981] found a tendency for the proton temperature to increase at some of the crossings of the nominal magnetic equator during the Voyager 1 encounter, while there was no such tendency on Voyager 2 inbound. The "background" temperature was $\sim 30 \text{ keV}$ at distances $\leq 40 R_J$ inbound during both encounters. Such behavior does not follow from an expansion during the Voyager 1 encounter unless the particles were energized during the rapid compression and retained their energy during the gradual expansion, just the opposite of adiabatic behavior.

The cold plasma component sampled by the PLS experiment does, however, show the qualitative effect of adiabatic expansion and compression. As noted previously, the plasma temperature of the cold component was $\sim 100 \text{ eV}$ on the dayside of the planet during both encounters, with the exception of the plasma sheet crossings by Voyager 1. At these crossings the plasma is about a factor of 10 colder. The magnetic field during the Voyager 1 encounter is not lower by a factor of 10 at the same radial distance from the planet, but, depending upon the field configuration and plasma location before the expansion (compression), simple adiabatic cooling in an expanding magnetosphere may give a partial explanation for the temperatures found in the plasma sheet by the PLS instrument on Voyager 1.

SUMMARY AND CONCLUSIONS

We have reexamined the plasma data obtained by the Voyager 2 spacecraft in the vicinity of Ganymede. We have shown that the plasma velocity, particularly the radial component, is too low to explain the series of observed plasma depletions as a wakelike structure produced by Ganymede and convected past the spacecraft. In addition, association of the depletions with Ganymede via the elongated magnetic field lines of the magnetosphere can also be ruled out on geometrical grounds.

The spatial location of the depletions suggests that they are a manifestation of an intermittent plasma instability, similar to ballooning modes occurring at the upper edge of the "second instability region" which can be excited in high- β , magnetically confined, laboratory plasmas. We have presented a mathematical model to illustrate the effects of such an instability in the context of the high- β plasma of the Jovian magnetosphere. In this case we argue that the plasma outflow from the Jovian magnetosphere allowed, for instance, by

resistive modes, is too slow to prevent the formation of sharp pressure gradients. These gradients, in turn, lead to the triggering of larger-scale ideal MHD modes.

The presence of an inward plasma flow throughout the region of interest led to a search for the origin of the motion and the possible connection between it and the coincidental location of the spacecraft near Ganymede while the instability was operative. Although most of this motion is field aligned and a similar flow pattern occurred during the Voyager 1 encounter, we have identified a rapid increase in the ram pressure of the solar wind against the magnetosphere during the Voyager 2 encounter, which rapidly, in turn, compressed the magnetosphere. The main effect of this compression was apparently to increase the plasma pressure gradient across the magnetic field. Conversely, we suggest that the Jovian magnetosphere underwent an expansion during the Voyager 1 encounter. This accounts for the lack of plasma depletions and, qualitatively, for the lower temperatures seen in the PLS data (positive ions and electrons) at that time.

During both encounters the "pooling" of relatively cold plasma results in a significant variation in the Alfvén speed along closed magnetic field lines. This is one of the features that makes it difficult to envision the onset of unstable, long-wavelength interchange perturbations. Especially in the plasma regime encountered by Voyager 1, microinstabilities (producing an anomalous resistivity) can develop which allow plasma to slip through the closed magnetic field lines and be unloaded in a quasi-continuous fashion. We suggest that this process, rather than the large scale interchange of magnetic flux tubes, is the dominant means of plasma loss in the middle magnetosphere, proceeding in a manner similar to the loss of thermal energy and particles observed in macroscopically stable, magnetically confined plasmas in the laboratory.

It is worth noting that Figures 8 and 9 show that for a substantial fraction of the time, the solar wind conditions can be quite steady. If the relaxation time of the magnetosphere is short compared to the interval between pressure increases, the Jovian magnetosphere may settle to states of quasi-equilibrium. It just happened that data on all of the plasma populations close to the planet were not gathered during such a time. Without better (fully self-consistent) models of the magnetosphere, it is difficult to assess how important the dynamic changes are as compared to models based upon a series of quasi-static equilibria.

Our analysis has indicated that at Jupiter, as at Earth, the upstream solar wind conditions can play a major role in determining magnetospheric conditions, configuration, and dynamics. A quantitative assessment of this magnetospheric input always requires two spacecraft. In the future, the Galileo orbiter spacecraft will be within the Jovian magnetosphere. Although there is no dedicated solar wind monitor in near-Jupiter space, the Ulysses spacecraft may be capable of fulfilling such a role, depending upon its launch date and arrival date at Jupiter as compared to those of Galileo. We predict that the depletions should be a reasonably frequent phenomenon and not be associated with Ganymede. The Galileo and Ulysses spacecraft could be used to test this hypothesis if there is sufficient coordination between the two missions.

Acknowledgments. We thank A. Pradhan for calculating solar wind conditions at each Voyager spacecraft based upon the in situ measurements at the other and the Voyager magnetometer team (N. Ness, principal investigator) for the magnetometer data displayed in Figure 6. Our sincere thanks go also to H. S. Bridge without whom

there would be no PLS data to analyze, to J. W. Belcher for both the initial suggestion of this project and constructive comments, to J. J. Ramos for proposing the model potential function (12), and to S. Migliuolo and G. Crew for their comments. R. L. McNutt, Jr., R. S. Selesnick, and P. S. Coppi were supported under NASA contract 953733 to the Jet Propulsion Laboratory.

The Editor thanks A. Eviatar and C. K. Goertz for their assistance in evaluating this paper.

REFERENCES

- Abe, T., and A. Nishida, Anomalous outward diffusion and associated heating of Iogenic ions in the Jovian magnetosphere, *J. Geophys. Res.*, **91**, 10003-10011, 1986.
- Armstrong, T. P., M. T. Paonessa, S. T. Brandon, S. M. Krimigis, and L. J. Lanzerotti, Low-energy charged particle observations in the 5-20 RJ region of the Jovian magnetosphere, *J. Geophys. Res.*, **86**, 8343-8355, 1981.
- Bagenal, F., Plasma conditions inside Io's orbit: Voyager measurements, *J. Geophys. Res.*, **90**, 311-324, 1985.
- Bagenal, F., and J. D. Sullivan, Direct plasma measurements in the Io torus and inner magnetosphere of Jupiter, *J. Geophys. Res.*, **86**, 8447-8466, 1981.
- Barbosa, D. D., D. A. Gurnett, W. S. Kurth, and F. L. Scarf, Structure and properties of Jupiter's magnetoplasma disc, *Geophys. Res. Lett.*, **6**, 785-788, 1979.
- Barnett, A., The response function of the Voyager plasma science experiment, *Tech. Rep. CSR-TR-84-1*, Mass. Inst. of Technol. Center for Space Res., Cambridge, 1984.
- Barnett, A., In situ measurements of the plasma bulk velocity near the Io flux tube, *J. Geophys. Res.*, **91**, 3011-3019, 1986.
- Barnett, A., and S. Olbert, The response function of modulator grid Faraday cup plasma instruments, *Rev. Sci. Instrum.*, **57**, 2432-2440, 1986.
- Basu, B., and B. Coppi, Localized plasma depletion in the ionosphere and the equatorial spread F, *Geophys. Res. Lett.*, **10**, 900-903, 1983.
- Belcher, J. W., and R. L. McNutt, Jr., The dynamic expansion and contraction of the Jovian plasma sheet, *Nature*, **287**, 813-815, 1980.
- Bridge, H. S., J. W. Belcher, R. J. Butler, A. J. Lazarus, A. M. Mavretic, J. D. Sullivan, G. L. Siscoe, and V. M. Vasylunas, The plasma experiment on the 1977 Voyager mission, *Space Sci. Rev.*, **21**, 259-287, 1977.
- Bridge, H. S., J. W. Belcher, A. J. Lazarus, J. D. Sullivan, R. L. McNutt, F. Bagenal, J. D. Scudder, E. C. Sittler, G. L. Siscoe, V. M. Vasylunas, C. K. Goertz, and C. M. Yeates, Plasma observations near Jupiter: Initial results from Voyager 1, *Science*, **204**, 987-991, 1979a.
- Bridge, H. S., J. W. Belcher, A. J. Lazarus, J. D. Sullivan, F. Bagenal, R. L. McNutt, Jr., K. W. Ogilvie, J. D. Scudder, E. C. Sittler, V. M. Vasylunas, and C. K. Goertz, Plasma observations near Jupiter: Initial results from Voyager 2, *Science*, **206**, 972-976, 1979b.
- Broadfoot, A. L., B. R. Sandel, D. E. Shemansky, J., C. McConnell, G. R. Smith, J. B. Holberg, S. K. Atreya, T. M. Donahue, D. F. Strobel, and J. L. Bertaux, Overview of the Voyager ultraviolet spectrometry results through Jupiter encounter, *J. Geophys. Res.*, **86**, 8259-8284, 1981.
- Burlaga, L. F., J. W. Belcher, and N. F. Ness, Disturbances observed near Ganymede by Voyager 2, *Geophys. Res. Lett.*, **7**, 21-24, 1980.
- Cheng, A. F., Magnetospheric interchange instability, *J. Geophys. Res.*, **90**, 9900-9904, 1985.
- Connerney, J. E. P., M. H. Acuña, and N. F. Ness, Modeling the Jovian current sheet and inner magnetosphere, *J. Geophys. Res.*, **86**, 8370-8384, 1981.
- Connerney, J. E. P., M. H. Acuña, and N. F. Ness, Voyager 1 assessment of Jupiter's planetary magnetic field, *J. Geophys. Res.*, **86**, 3623-3627, 1982.
- Coppi, B., Plasma collective modes involving geometry and velocity spaces, in *Advances in Plasma Physics*, vol. 4, edited by A. Simon and W. B. Thompson, Wiley-Interscience, New York, 1971.
- Coppi, B., and R. L. McNutt, Jr., Plasma voids and the bubbling model of Jupiter's magnetosphere, *Eos Trans. AGU*, **66**, 341, 1985.
- Coppi, B., and M. N. Rosenbluth, Collisional interchange instabilities in shear and $\int dl/B$ stabilized systems, *Plasma Phys. Controlled Nucl. Fusion Res. Proc. Conf.*, **2**, 1966.
- Coppi, B., M. N. Rosenbluth, and S. Yoshikawa, Localized (ballooning) modes in multipole configurations, *Phys. Rev. Lett.*, **20**, 190-192, 1968.

- Coppi, B., J. Filreis, and F. Pegoraro, Analytical representation and physics of ballooning modes, *Ann. Phys. NY*, 121, 1-31, 1979a.
- Coppi, B., A. Ferreira, J. W. -K. Mark, and J. J. Ramos, Ideal-MHD stability of finite-beta plasmas, *Nucl. Fusion*, 19, 715-725, 1979b.
- Fejer, B. G., and M. C. Kelly, Ionospheric irregularities, *Rev. Geophys.*, 18, 401-454, 1980.
- Gazis, P. R., Observations of plasma bulk parameters and the energy balance of the solar wind between 1 and 10 AU, *J. Geophys. Res.*, 89, 775-785, 1984.
- Hairston, M. R., and T. W. Hill, Jovian ionospheric conductivity and magnetospheric plasma outflow: Voyager 1, *J. Geophys. Res.*, 90, 9889-9892, 1985.
- Hasegawa, A., Ballooning instability and plasma density limitations in Jovian magnetosphere, paper presented at Conference on Physics of the Jovian Magnetosphere, Rice Univ., Houston, Tex., 1980.
- Hill, T. W., Inertial limit on corotation, *J. Geophys. Res.*, 84, 6554-6558, 1979.
- Hill, T. W., A. J. Dessler, and F. C. Michel, Configuration of the Jovian magnetosphere, *Geophys. Res. Lett.*, 1, 3-6, 1974.
- Hill, T. W., A. J. Dessler, and C. K. Goertz, Magnetospheric models, in *Physics of the Jovian Magnetosphere*, edited by A. J. Dessler, Chap. 10, Cambridge University Press, New York, 1983.
- Khurana, K. K., and M. G. Kivelson, A reanalysis of Voyager 2 magnetic data in the "Ganymede wake" region, *Eos Trans. AGU*, 66, 1049, 1985.
- Khurana, K. K., M. G. Kivelson, R. J. Walker, and T. P. Armstrong, A reanalysis of Voyager 2 field and particle data near Ganymede's orbit, paper presented at Second Neil Brice Memorial Symposium on Magnetospheres of the Outer Planets, Iowa City, Iowa, Sept. 1-5, 1986.
- Krimigis, S. M., T. P. Armstrong, W. I. Axford, C. O. Bostrom, C. Y. Fan, G. Gloeckler, L. J. Lanzerotti, E. P. Keath, R. D. Zwickl, J. F. Carbary, and D. C. Hamilton, Hot plasma environment at Jupiter: Voyager 2 results, *Science*, 206, 977-984, 1979.
- Krimigis, S. M., J. F. Carbary, E. P. Keath, C. O. Bostrom, W. I. Axford, G. Gloeckler, L. J. Lanzerotti, and T. P. Armstrong, Characteristics of hot plasma in the Jovian magnetosphere: Results from the Voyager spacecraft, *J. Geophys. Res.*, 86, 8227-8257, 1981.
- Lazarus, A. J. and R. L. McNutt, Jr., Low-energy plasma observations in Saturn's magnetosphere, *J. Geophys. Res.*, 88, 8831-8846, 1983.
- McNutt, R. L., Jr., The dynamics of the low energy plasma in the Jovian magnetosphere, Ph.D. thesis, Mass. Inst. of Technol., Cambridge, 1980.
- McNutt, R. L., Jr., Possible *in situ* detection of K^{2+} in the Jovian magnetosphere, *Eos Trans. AGU*, 63, 1062, 1982.
- McNutt, R. L., Jr., Force balance in the magnetospheres of Jupiter and Saturn, *Adv. Space Res.*, 3, 55-58, 1983.
- McNutt, R. L., Jr., Force balance in outer planet magnetospheres, in *SP1 Conference Proceedings and Reprint Series, 5, Proceedings of the 1982-4 MIT Symposia on the Physics of Space Plasmas*, edited by J. Belcher, H. Bridge, T. Chang, B. Coppi, and J. R. Jasperse, Scientific Publishers, Cambridge, Mass., 1984.
- McNutt, R. L., Jr., J. W. Belcher, and H. S. Bridge, Positive ion observations in the middle magnetosphere of Jupiter, *J. Geophys. Res.*, 86, 8319-8342, 1981.
- McNutt, R. L., Jr., P. S. Coppi, R. S. Selesnick, and J. W. Belcher, Further analysis of the "Ganymede wake" observations, *Eos Trans. AGU*, 66, 341, 1985.
- Ness, N. F., M. H. Acuña, R. P. Lepping, L. F. Burlaga, K. W. Behannon, and F. M. Neubauer, Magnetic field studies at Jupiter by Voyager 2: Preliminary results, *Science*, 206, 966-972, 1979.
- Richardson, J. D., Thermal ions at Saturn: Plasma parameters and implications, *J. Geophys. Res.*, 91, 1381-1389, 1986.
- Ramos, J. J., General equilibrium and stability properties of high beta tokamaks, *Phys. Fluids*, 27, 2313-2318, 1984.
- Sands, M. R., Field aligned flows in Jupiter's dayside middle magnetosphere, *Eos Trans. AGU*, 65, 1038, 1984.
- Siscoe, G. L. and D. Summers, Centrifugally driven diffusion of Iogenic plasma, *J. Geophys. Res.*, 86, 8471-8479, 1981.
- Slavin, J. A., E. J. Smith, J. R. Spreiter, and S. S. Stahara, Solar wind flow about the outer planets: Gas dynamic modeling of the Jupiter and Saturn bow shocks, *J. Geophys. Res.*, 90, 6275-6286, 1985.
- Smith, E. J., R. W. Fillius, and J. H. Wolfe, Compression of Jupiter's magnetosphere by the solar wind, *J. Geophys. Res.*, 83, 4733-4742, 1978.
- Summers, D., and G. L. Siscoe, Wave modes of the Io plasma torus, *Astrophys. J.*, 295, 678-684, 1985.
- Tariq, G. F., T. P. Armstrong, and T. H. Collision, Voyager 2 observations of energetic particle variations in the Ganymede wake region: A possible acceleration mechanism, *J. Geophys. Res.*, 88, 5551-5563, 1983.
- Tariq, G. F., T. P. Armstrong, and J. W. Lowry, Electrodynamic interaction of Ganymede with the Jovian magnetosphere and the radial spread of wake-associated disturbances, *J. Geophys. Res.*, 90, 3995-4009, 1985.
- Vasyliunas, V. M., Plasma distribution and flow, in *Physics of the Jovian Magnetosphere*, edited by A. J. Dessler, Chap. 11, Cambridge University Press, New York, 1983.
- Wolff, R. S., and D. A. Mendis, On the nature of the interaction of the Jovian magnetosphere with the icy Galilean satellites, *J. Geophys. Res.*, 88, 4749-4769, 1983.
- Zalesak, S. T., S. L. Ossakow, and P. K. Chaturvedi, Nonlinear equatorial spread F: The effect of neutral winds and background Pedersen conductivity, *J. Geophys. Res.*, 87, 151-166, 1982.

B. Coppi, P. S. Coppi, R. L. McNutt, Jr., and R. S. Selesnick, Center for Space Research, Massachusetts Institute of Technology, 37-635, 77 Mass. Ave., Cambridge, MA 02139.

(Received July 3, 1986;
revised December 5, 1986;
accepted January 15, 1987)